4-2012

Error Reduction and Effect of Step Size in Adjustment Calculus for Cam Applications

Sai Siddhartha Nudurupati
University of Nebraska-Lincoln, saisiddu@gmail.com

ERROR REDUCTION AND EFFECT OF STEP SIZE IN ADJUSTMENT CALCULUS FOR CAM APPLICATIONS

by

Sai Siddhartha Nudurupati

A THESIS

Presented to the Faculty of

The Graduate College at the University of Nebraska

In Partial Fulfillment of Requirements

For the Degree of Master of Science

Major: Mechanical Engineering

Under the Supervision of Professor Wieslaw M. Szydlowski

Lincoln, Nebraska

April, 2012

ERROR REDUCTION AND EFFECT OF STEP SIZE IN ADJUSTMENT CALCULUS FOR CAM APPLICATIONS

Sai Siddhartha Nudurupati, M.S.

University of Nebraska, 2012

Adviser: Wieslaw M. Szydlowski

Any measurement, however carefully done, will never be free from errors. Similarly, machining of cams for automobiles is prone to contain errors. These errors are naturally a part and parcel of cam manufacturing. The nature of deviations of the manufactured cam profile from the theoretical cam determines its usability. Sometimes, allowable deviations in high speed cams may be in the order of 2540 μm. Larger deviations will disqualify the cams for applications.

Velocity and acceleration of the cam are estimated from the measured displacement of the cam follower during quality control implementation. This data helps in eliminating the unfit cams. Existing methods deal with a notorious challenge from propagation of measurement errors in the displacement data to predicted velocity and acceleration values.

J. Oderfeld developed a little known method called ‘Adjustment Calculus’ which is an alternative method for this purpose. This method combines the ‘marching point’

method that fits a polynomial to discrete data and a symmetric Stirling interpolation method. Until now, adjustment calculus has been applied to reduce errors in acceleration data. In this work, adjustment calculus is implemented to velocity predictions. ‘Weights’ for calculation of adjusted velocity are derived using a cubic polynomial fit and symmetric Stirling interpolation formula. The effect of step size on application of adjustment calculus to different cam profiles is probed using the Monte Carlo method.

Effective step size for practical applications in automotive cam quality control is suggested for each cam profile. Practical pointers for application to cam inspection for velocity and acceleration analysis are formulated.

Table of Contents

ACKNOWLEDGMENT

I wanted to express my sincere gratitude to Dr. Wieslaw M. Szydlowski for his encouragement, guidance and patience while supervising my thesis. I have been an admirer of his knowledge in engineering and teaching methods from his first course Intermediate Kinematics that I have attended. I am also grateful to Dr. Carl Nelson and Dr. Linxia Gu for their support and assistance.

I wanted to express extreme gratitude to my parents Sri N. S. S. Sai and Smt. N. Sarada and my sister N. Sai Sravanthi for their love and support throughout my life. I want to thank Dr. Arun Natarajan for his invaluable advice and guidance. I would like to thank my friends Satish, Padma, Apoorva, Chaitanya, Dhairya, Hardik, Shailesh, Uday, Ke, Chris, Sri Harsha, Venkat, Ananth, Mahanth and Ved who have been very supportive and encouraging.

I would like to prostrate to Shri Sai Baba for this life and beyond.

LIST OF TABLES

LIST OF FIGURES

1. INTRODUCTION

1.1 Role of Errors in Engineering Process

Any measurement, however carefully done, will never be free from errors. ‘Error’ does not carry the same connotation as ‘mistake’ or ‘blunder’ in science. In scientific applications, ‘error’ refers to the inevitable deviation from true value. Errors cannot be eliminated but can be controlled to be reasonably small in magnitude [1]. Errors can be produced due to various factors. Faulty setup, wear of the tools and fixtures, vibrations and rise of temperature due to machining are few of them. Many times, round off by computerized devices causes errors that can be treated as random variables. These random errors tend to follow a certain distribution. All machining operations produce errors that are statistical phenomena. They can be estimated using probabilistic techniques [2].

1.2 Special Role of Cam Mechanisms

Cam-follower mechanisms are simple and cheap mechanisms that are widely used in machinery. The cam and follower are machine elements that comprise the cam-follower mechanisms. The cam drives the follower. These mechanisms are often compact and highly reliable as they contain few moving parts. In a typical cam-follower mechanism, the follower rests on the face of a cam. The cam undergoes rotary motion which is converted to cyclic translatory motion of the spring-loaded follower due to direct contact. Motion of the follower is thus highly influenced by the shape and surface profiles of the cam and follower. Therefore, it is absolutely important to understand the relationship between follower motion and the cam profile [2][3]. Cams can be classified based on their basic shapes as:

a) Plate cam
b) Wedge cam
c) Cylindric cam
d) End cam

Similarly, follower can be classified based on their basic shape as;

a) Knife-edge follower
b) Flat-face follower
c) Roller follower
d) Spherical-face or curved-shoe follower

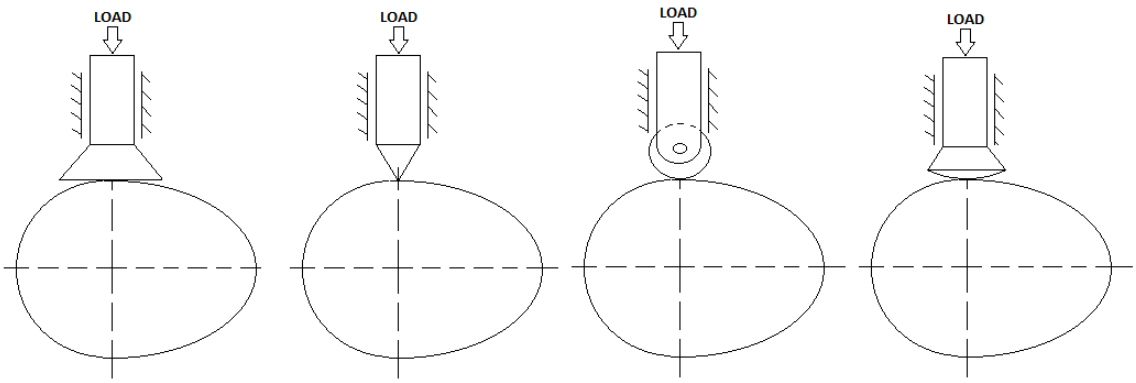

Figure 1.2.1: (a) Flat-face follower (b) Knife-edge follower (c) Roller follower (d) Spherical-face follower [16]

Cam mechanisms find applications in internal combustion engines of automobiles, transportation equipment, textiles, machine tools, printing presses, switches, ejection molds, control systems, packaging and recently in micro-electromechanical systems [2].

1.2.1 Manufactured Cam-Follower System Errors

Cams are machined with great care as it is of prime importance to achieve a smooth cam profile. Cams are manufactured in high volumes using manual or numerical control (NC) machining, analog duplication of a hand dressed master cam, computer numerical machining (CNC), electro-discharge machining (EDM) or other methods such as flame cutting, die casting, die forging, stamping and powder metallurgy [2].

Errors are inherent in manufactured cam-follower systems. For satisfactory functioning of these systems, these errors should be minimized. These errors are defined as the deviations of performance of cam-follower system from desired theoretical characteristics. These errors can be classified as follows [2]:

1.2.1.1 Structural Errors

These errors arise from use of faulty dimensions, wrong parts, mistakes in the inputs to the machining equipment or the assembly, programming errors, etc..

1.2.1.2 Fixed Backlash Errors

These errors are common in cam follower systems. There is a need to reduce these errors through improvised designs. These errors are caused due to the clearances which are unavoidable such as the ones between follower and cam groove.

1.2.1.3 Variable Backlash Errors

Tolerances are inherent to all manufactured parts. These tolerances are the cause for unintended clearances that are variable. These additional clearances cause variable backlash errors. It is reckoned that these clearances are normally distributed. Thus this understanding can be extrapolated to the distribution of variable backlash errors.

1.2.1.4 Cyclic Errors

Rotating elements deal with the concern of wobbling due to eccentricities. Cams especially are eccentric by nature. These eccentricities cause errors called cyclic errors.

1.2.1.5 Cam Profile Errors

After machining, cam profiles are compared to the theoretical cam curves. The deviations from theoretical curves cause these errors. Machining events like filing, improper milling or wear of grinding tools can cause these errors. Machine shop's expertise is of vital importance in tackling these errors. It has been observed that the 'blip' that occurs in the acceleration curve is caused due to the erroneous start and stop of the grinding wheel.

1.2.1.6 Waviness

'Waviness' varies from 'roughness' marginally with longer lengths between peaks and valleys. Increased feed on the milling cutter while machining can cause it. Waviness causes undesirable jumps in acceleration.

1.2.2 Generalized Classification of Errors

As discussed earlier, manufacturing errors follow a certain statistical trend. To facilitate analysis, all the errors are classified into two groups as systematic errors and random errors.

1.2.2.1 Systematic Errors:

Some errors are inherent in the system and are consistently repeated every time the measurement is performed with the same setup. Likewise, interpolation methods introduce their own systematic errors. In these cases, an approximation error will significantly contribute towards systematic error. For example, a cubic polynomial can be used to approximate a cosine function. At a certain value of the angle both the curves would have a common point but their slopes would vary at that point.

1.2.2.2 Random Errors:

These errors are inconsistent in nature. These arise from improper measurement technique, poor precision, wear of measuring instruments, etc.. It has been observed that these errors are stochastic in nature. These errors are approximated using statistical procedures. During analysis, it is assumed that random errors follow a normal distribution. In this work, random errors will be approximated to follow the normal distribution with a specified standard deviation. Computer software will be used to

approximate random errors to simulate the estimations of velocity and acceleration from displacement data of cam follower systems [4].

1.3 Need to determine "True Acceleration" from measured data

1.3.1 Intelligent robots with vision

Currently, robots are equipped with vision systems which would track movements of a body or a point. These robots are programmed to move their end effectors to the desired locations based on the data received from the vision systems. Therefore, accurate estimations of velocity and acceleration of the data points are desired from the measurements of displacement made at equal intervals of time. These velocity and acceleration values will effect the final position of the end effectors [5].

1.3.2 Manufacture of missile shells

Missile shells have a meticulous profile for the outer shell. These missiles might travel at super-sonic speeds when fired. The outer shells need to have a very smooth finish to reduce drag resistance during flight. Robotic arms are used to meticulously finish the complex profile of the outer shell. This profile is fed into the computers that control the robot's end effectors. Estimations of velocities and accelerations of the end effectors are made by the computer based on the input profile data. Adjustment calculus has the potential to reduce the errors in these estimations of velocity and acceleration.

1.3.3 Diagnostics of hand-arm vibration syndrome

Hand-arm vibration syndrome (HAVS) is an occupational disease. It is caused by prolonged exposure to vibration of power tools [6]. Fingers, hands and forearms are

affected by this disease. Measuring systems used in diagnosis of this disease are equipped with vibrometer units which record acceleration data. This acceleration data is interpreted in terms of thresholds to diagnose the disease [7].

1.3.4 Position Tracking of Mechanical Linkages:

In applications like tracking position of mechanical linkages during arthroscopic hip surgery [8], kinematic analysis of three dimensional motions [9] and nonlinear array algebra in digital photogrammetry [10], displacement data is used to interpret acceleration data. Therefore, acceleration data is calculated from measured displacement data.

1.3.5 Musculoskeletal analysis of race horse:

Distances cantered by the race horses were quantified and interpreted in terms of velocities and accelerations to study the effects of workload, nutrition and work environment of race horses. Motion of the limbs of race horses was studied by sensors attached at different locations. Velocity and acceleration values were then interpreted from this data [11].

1.3.6 Cam's velocity and acceleration estimation:

Cams which comprise cam-follower systems are designed to follow a prescribed path. It is desirable to know how velocity and acceleration of the follower varies over the motion. This information is of critical importance in high speed applications. It is a common practice to determine velocity and acceleration values from displacement data [12].

1.4 Need for numerical differentiation & integration

Section 1.3 deals with the necessity of determination of velocity and acceleration data from displacement data. Numerical calculus, which deals with numerical differentiation and integration, offers an approximate but simple solution for this purpose. Displacement data can be manipulated mathematically using numerical calculus to find velocity and acceleration data. This data might be an approximation but often serves the purpose if properly implemented. The main advantage of numerical calculus is that it can be readily applied. It can be implemented to predict velocities and accelerations accurately especially when accelerometers struggle with noise [12].

1.5 Current Methods

Errors caused while manufacturing the cam affect its profile and thus deviates the displacement curve relative to the theoretical curve. These deviations adversely affect the velocity and acceleration curves [13][14][15]. A common practice in such situations is to smooth out the velocity and acceleration curves by making small adjustments such that original curve is not influenced greatly. This technique is generally referred to as "Curve Smoothing" or "Curve Adjustment" [16].

1.5.1 Finite differences:

Taylor series expansion for a function y = y(x) whose derivatives are continuous can be written as

$$y(x+\Delta x) = y(x) + (\Delta x)\dot{y}(x) + \frac{(\Delta x)^2}{2!}\ddot{y}(x) + \frac{(\Delta x)^3}{3!}\dddot{y}(x) + \ldots,$$

Eq. 1.5.1.1

Here, the dots represent differentiation with respect to x. If terms containing $\ddot{y}(x)$ and higher are not included, then the approximation is valid up to second order. The accuracy of the above approximation increases with increased number of terms.

In Figure 1.5.1.1, a small equally spaced increment of Δx is represented by 'h'. An independent variable x_i is considered. The corresponding dependent variable is y_i. Neighboring points on the abscissa to the left of x_i are designated by $x_{i-1}, x_{i-2}, \ldots$ etc. and to the right by $x_{i+1}, x_{i+2}, \ldots$ etc.. Corresponding ordinates are designated by $y_{i-1}, y_{i-2}, \ldots$ etc. and $y_{i+1}, y_{i+2}, \ldots$ etc respectively. Using this notations, the Taylor's expansion (Eq. 1.5.1) can be written as,

$$y_{i+1} = y_i + h\dot{y}_i + \frac{h^2}{2!}\ddot{y}_i + \ldots$$

Eq. 1.5.1.2

Similarly,

$$y_{i-1} = y_i - h\dot{y}_i + \frac{h^2}{2!}\ddot{y}_i - \ldots$$

Eq. 1.5.1.3

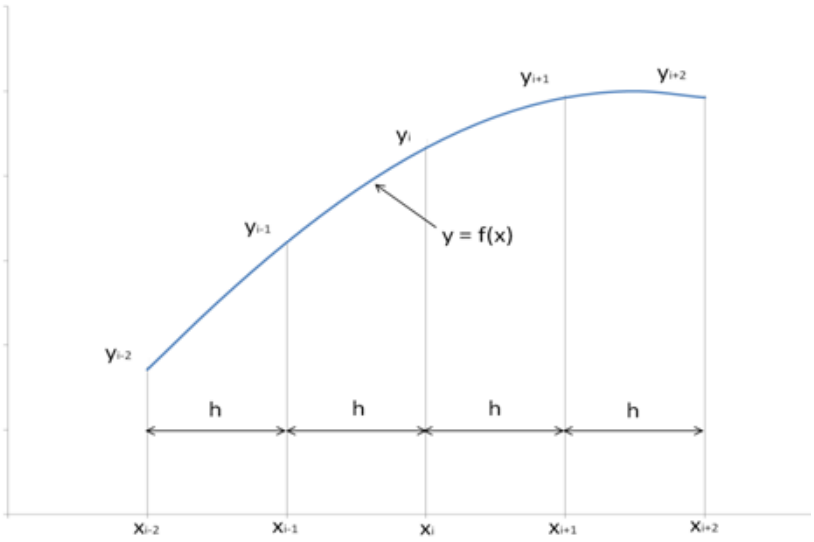

Figure 1.5.1.1: Application of Finite Differences [16]

Here, the higher order terms are ignored. By combining Eqs. 1.2.2 and 1.2.3, we get

$$\dot{y}_i = \frac{1}{2h} y_i'$$

Eq. 1.5.1.4

And

$$\ddot{y}_i = \frac{1}{h^2} y_i''$$

Eq. 1.5.1.5

Where,

$$y_i' = y_{i+1} - y_{i-1}$$

Eq. 1.5.1.6

And

$$y_i'' = y_{i-1} - 2y_i + y_{i+1}$$

Eq. 1.5.1.7

Equations (1.2.4) and (1.2.5) represent the central approximations of second order for first derivative (velocity) and second derivative (acceleration) of any function represented by a set of discrete data. y_i' can be called the velocity factor and y_i'' can be called the acceleration factor.

Considering an equally spaced discrete function, a difference table can be written as

Table 1.5.1.1: Difference Table

x_0	y_0				
		Δy_0			
x_1	y_1		$\Delta^2 y_0$		
		Δy_1		$\Delta^3 y_0$	
x_2	y_2		$\Delta^2 y_1$		$\Delta^4 y_0$
		Δy_2		$\Delta^3 y_1$	
x_3	y_3		$\Delta^2 y_2$		
		Δy_3			
x_4	y_4				

Difference tables simplify the process of calculating higher order differences. In the above table, diagonal components evaluate the difference in values of neighboring cells on the left. For example,

$$\Delta y_m = y_{m+1} - y_m$$

Eq. 1.5.1.8

Δy_m is called a first difference. These values of first difference are proportional to velocity and thus can be employed to determine velocity from displacement data [16]. Differences of Δy_m values are called second differences and are denoted by $\Delta^2 y_m$ and equals

$$\Delta^2 y_m = \Delta y_{m+1} - \Delta y_m$$

Eq. 1.5.1.9

Similarly, second difference values are proportional to acceleration. Therefore, these values can be used to determine acceleration from displacement data [16]. 'nth' order differences can be written as

$$\Delta^n y_m = \Delta^{n-1} y_{m+1} - \Delta^{n-1} y_m$$

Eq. 1.5.1.10

1.5.2 Johnson's Method:

Johnson's method [12] is a trial and error method used to smoothen the acceleration plot. Using the measured displacement values of the follower, the corresponding acceleration factors y_i'' can be calculated. The acceleration factors thus obtained contain lot of fluctuations. In some cases, these fluctuations alter the acceleration plot beyond recognition.

To obtain the acceleration curve that is close to the real curve, the fluctuations have to be lessened or removed (ideally). This is done by altering the displacement value of the points whose corresponding acceleration factors deviate from the acceleration curve. For every alteration in the displacement value, three acceleration values have to be changed. For example, let y_i be the ith displacement value and y_i'' is the corresponding acceleration factor. If y_i is modified by a value 'k', y_i'' has to be corrected by a value of '-2k' and $y_{i+1}'' \& y_{i-1}''$ have to be corrected by a value 'k'. Points have to be traversed

sequentially, modifying the displacements based on the effect of the modifications on the acceleration curve. Several traversals are required to get the desired acceleration curve. In every traversal, displacement values have to be carefully modified to avoid excessive divulgence from the initial displacements. The results of this method are dependent on experience of the user who is introducing changes to the recorded displacements. Excessive divergence from the initial displacement would result in a huge acceleration factor at the end of the traversal. It is difficult to formulate a software code to automate such procedures.

Table 1.5.2.1 presents a numerical example for application of Johnson's method on the given data of cam-follower displacement data. The first column consists of the cam position (θ) in degrees. The second column contains follower displacement data at corresponding 'θ'. Initial acceleration factors are calculated first. Where acceleration factors can be calculated as:

$$AF = S_{i-1} + S_{i+1} - 2S_i$$

Eq. 1.5.2.1

Now, displacements have to be adjusted for the values whose acceleration factors deviate a lot. Three traversals are made in this example. The fourth traversal is done to slightly adjust the resultant acceleration curve further. The first traversal is started at displacement corresponding to 4º position. Displacement data is adjusted by '+2540'. Once the displacement data is adjusted, its corresponding acceleration factor is adjusted by (-2) times the value used for adjustment as shown in column 1.1 corresponding to 4º position. Correction factors corresponding to 2º position and 6º position are each adjusted

by (+1) times the values used for adjusting the displacement of 4 º position. This procedure is carried out for rest of the positions until the completion of this traversal.

The second traversal is started at 16º position and the third traverse is started at 14º position. It can be observed that a minimum level of skill is required to apply this procedure efficiently with lesser number of traversals as it is a trial-and-error procedure. Also, it is extremely complicated to develop an algorithm that can be implemented using software for the application of such methods.

Table 1.5.2.1: An Example for Application of Johnson's method

Cam Position (Theta)	Initial Follower displacement	Displ. Adjustments (mm*10^5)				Initial Accel. factors (*10^5)	Corrected Acceleration Factors (*10^5)									
							1			2			3			4
(deg.)	mm*10^5	1	2	3	4	S1+S2-2S0	1.1	1.2	1.3	2.1	2.2	2.3	3.1	3.2	3.3	4.1
0	2540000	*				0										
2	2544572	**				-4572	-2032									
4	2544572	2540				-4572	-9652	-4572								
6	2540000	5080				-4826	-2286	-12446	-6096							
8	2530602	6350				-4572	508	-12192	-6350							-6096
10	2516632	5842			254	-4826	1524	-10160	-5080							-5588
12	2497836	5080				-4572	1270	-8890	-4826				-5588			-5334
14	2474468	4064		-762		-4826	254	-7874	-4572	-5334			-3810	-4572		
16	2446274	3302	-762	-762		-4572	-508	-7112	-4572	-3048	-4826		-5588	-4064	-3556	
18	2413508	2540	-1778	508		-1016	2286	-2794	-1270	-2032	1524	-1016	-1778	-2794	-3810	
20	2379726	1524	-2540	1270		3302	5842	2794	2286	508	5588	10668	11176	8636	9398	
22	2349246	-508	-2540	762		4826	6350	7366	4826	2286	7366	4826	6096	4572	4572	
24	2323592	-2540	-2540	0		4572	4064	9144	5334	2794	7874	5080	5842	5842	5334	
26	2302510	-3810	-2794	-508		4572	2032	9652	5588	3048	8636	4826	4826	5842	5334	
28	2286000	-4064	-3810	-508		4826	1016	9144	5334	2540	10160	5080	4572	5588		
30	2274316	-3810	-5080			4572	508	8128	5080	1270	11430	6350	5842			6096
32	2267204	-3048	-5080		254	4826	1016	7112	5080	0	10160	6350				5842
34	2264918	-2032	-3810			4572	1524	5588	4572	-508	7112	5588				5842
36	2267204	-1016	-1524			4826	2794	4826		1016	4064					
38	2274316	**				4572	3556			2032						
40	2286000	*				0										

1.5.3 Polynomial Approximation:

Polynomial approximation [17] is one of the most common methods used for interpolation and extrapolation when values at discrete points (e.g., ‘m’ number of points) are known. The general equation used for this method is given as;

$$y = C_0 + C_1 x + C_2 x^2 + C_3 x^4 + \cdots + C_n x^n$$

Eq. 1.5.3.1

Where;

C_0, C_1, C_2… C_n – Coefficients of the polynomial used to fit the curve

The first question that is answered using this technique is the degree of the polynomial to be used for optimal approximation of the data. It is self evident that the degree of the polynomial is less than the number of points known. It is observed that a polynomial with a degree closer to the number of points ‘m’ will not result in a smooth curve. Also, such a curve would fluctuate tremendously between a pair of adjacent points. Therefore, a polynomial of a degree much less than the number of points ‘m’ is used. If a polynomial of very low degree is selected, the accuracy of approximation achieved might be insufficient. If a polynomial with a greater degree is selected, the computation time and memory space used might be affected adversely. This would be of concern if this procedure is used for enormous amounts of data and at high frequencies. Therefore, it is desired to select the degree of the polynomial optimally. Sometimes, the data may be associated with a hint about the polynomial that needs to be selected. Plots of the data at hand might suggest the appropriate degree to be selected. The most widely used method for this purpose is a statistical method based on standard deviation.

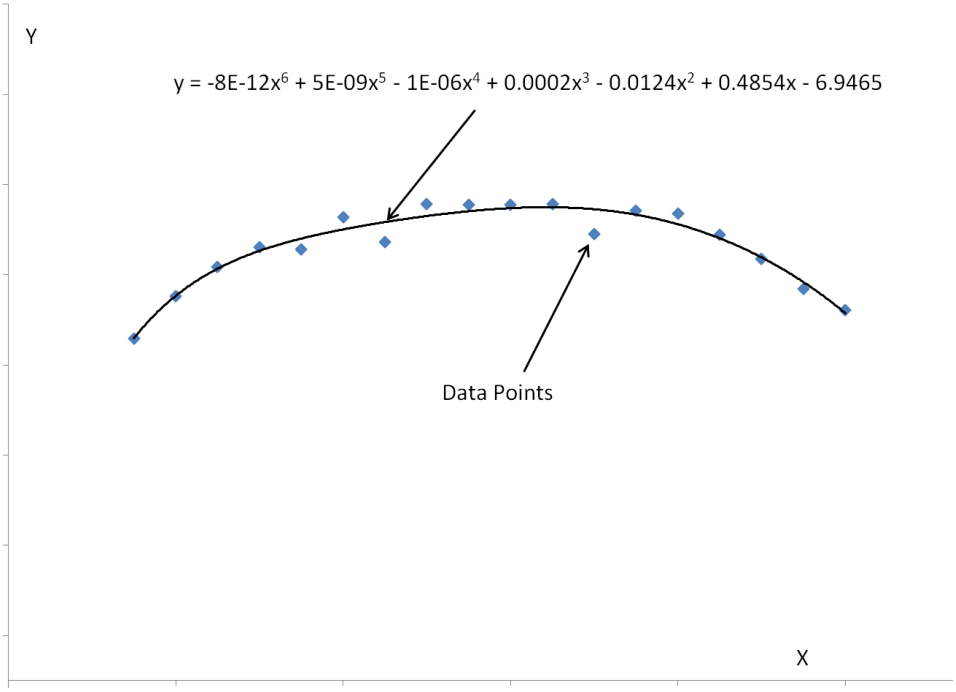

Figure 1.5.3.1: Example for Polynomial Approximation

'Standard error of estimate σ_e', which is used to find the degree of polynomial that fits the data, is defined as the quotient of the ratio of the sum of squares of deviations of data points from the corresponding points of the curve obtained to the degrees of freedom of fit. Degrees of freedom equals 'm-n-1' where 'm' is the number of data points known and 'n' equals the degree of polynomial. The standard error estimate is defined as;

$$\sigma_e = \sqrt{\frac{\sum_{i=1}^{m}(y(x_i) - y_i)}{m - n - 1}}$$

Eq. 1.5.3.2

Where:

y_i = y data values corresponding to x_i

$y(x_i)$ = y value of fitting curve at x_i

Polynomials with different degrees have to be tried and the value of 'σ_e' has to be calculated for every trial. Increased degree of polynomials does not necessarily provide lowered value of 'σ_e'. Statistical selection of the optimum degree can be based on two different criteria;

1. Highest degree polynomial with a 'statistically significant' reduction in 'σ_e' can be selected
2. Polynomial that yields greatest decrease in 'σ_e' from the polynomial one degree lower can be selected

Computers are usually used to implement this method. It can be inferred that this is a trial and error method and is dependent on the skill of the user in arriving at an appropriate degree efficiently. The results can be ambiguous at times.

1.5.4 Chen's Method:

Chen [18] developed numerical algorithms to synthesize cam displacement from a prescribed acceleration curve. His algorithms are not trial and error but are approximate in nature. These algorithms can be applied when an acceleration curve has been described discretely. They approximate the displacement data that satisfy the end conditions of motion based on the available acceleration data. His algorithms are based on the following derivation. From Eq. 1.5.1.7, the second difference y_i" can be defined as:

$$y_i'' = y_{i-1} - 2y_i + y_{i+1}$$

Eq. 1.5.4.1

Multiplying both sides of Eq. 1.5.4.1 by (N-i), where N is the final station of the final nodal point and i = 1, 2… (N-1) and summing up we get:

$$\sum_{i=1}^{N-1}(N-i)y_i'' = \sum_{i=1}^{N-1}(N-i)(y_{i-1} - 2y_i + y_{i+1})$$

Eq. 1.5.4.2

Right hand side of Eq. 1.5.4.2 can be expanded as follows:

$$\sum_{i=1}^{N-1}(N-i)(y_{i-1} - 2y_i + y_{i+1}) = \sum_{i=1}^{N-1}(N-i)y_{i-1}\, 2\sum_{i=1}^{N-1}(N-i)y_i + \sum_{i=1}^{N-1}(N-i)y_{i+1}$$

$$= (N-1)y_0 + (N-2)y_1 + (N-3)y_2 + \cdots + y_{N-2}$$

$$- 2[(N-1)y_1 + (N-2)y_2 + \cdots + 2y_{N-2} + y_{N-1}] + (N-1)y_2$$

$$+ (N-2)y_3 + \cdots + 2y_{N-1} + y_N$$

$$= (N-1)y_0 - Ny_1 + y_N$$

Eq. 1.5.4.3

$$y_1 = \frac{Ny_0 + h}{N} - \sum_{i=1}^{N-1}(N-i)y_i''$$

Eq. 1.5.4.4

Where:

y_0 = Initial reading of ordinate

y_N = Final reading of ordinate

h = Total lift of follower

From Eq. 1.5.4.1 and Eq. 1.5.4.4, we can write a sequence of equations

$$y_2 = -y_0 + 2y_1 + y_1''$$

$$y_3 = -y_1 + 2y_2 + y_2'' = -2y_0 + 3y_1 + (2y_1'' + y_1'')$$

$$y_4 = -y_2 + 2y_3 + y_3'' = -3y_0 + 4y_1 + (3y_1'' + 2y_2'' + y_3'')$$

...

...

Using mathematical induction;

$$y_n = (1-n)y_0 + ny_1 + \sum_{i=1}^{n-1}(n-i)y_i''$$

Eq. 1.5.4.5

Where:

n = 2, 3, 4… (N-1)

Eq. 1.5.4.4 and Eq. 1.5.4.5 form the basis for synthesis equations. It can be observed that a complex algorithm needs to be run to approximate the displacement data. This method duplicates the method of finite differences to estimate the velocities and accelerations from discrete displacement data.

1.5.5 Adjustment Calculus:

Adjustment calculus is a mathematical procedure which was proposed by J. Oderfeld [19]. This procedure can be interpreted as a sequence of two steps. The first step deals with smoothing the displacement curve by adjustment with the use of a cubic polynomial and the concept of "Marching Point". The second step involves computation of velocity and acceleration values using Stirlings interpolation formula for equidistant points. An attempt will be made to explain this procedure and demonstrate it with an example in this section. It is interesting to note here that a cubic polynomial is selected because the cubic polynomial is the lowest order polynomial which has an inflection point. Any higher order polynomial can be used to further explore this procedure.

Consider a point in three-dimensional space S(x,y,z) with x, y and z as its Cartesian coordinates defined by X, Y and Z axes respectively. Consider a path followed by this point in equal intervals of time 't'. Each position traversed by this point will have its own coordinates in the XYZ domain. To calculate the velocity and acceleration of this point, we will need to consider few positions. Let's consider the i^{th} position defined as $S_i(x_i, y_i, z_i)$. The coordinates of the $(i-1)^{th}$ and $(i+1)^{th}$ positions are $S_{i-1}(x_{i-1}, y_{i-1}, z_{i-1})$ and $S_{i+1}(x_{i+1}, y_{i+1}, z_{i+1})$ respectively.

The velocity of the point S at the i^{th} position can be written as a vector sum of velocity of x, y and z components:

$$\overline{V_i} = \overline{V_x} + \overline{V_y} + \overline{V_z}$$

Eq. 1.5.5.1

Therefore, the magnitude of the velocity can be written as;

$$V_i = \sqrt{V_x^2 + V_y^2 + V_z^2}$$

Eq. 1.5.5.2

Similarly, acceleration of $S_i(x_i, y_i, z_i)$ can represented as vector sum:

$$\overline{A_i} = \overline{A_x} + \overline{A_y} + \overline{A_z}$$

Eq. 1.5.5.3

Therefore, the magnitude of the acceleration can be written as:

$$A_i = \sqrt{A_x^2 + A_y^2 + A_z^2}$$

Eq. 1.5.5.4

Therefore, any motion in three dimensions can be thus studied through vector line analysis of the projections in the X, Y and Z axes.

Let's consider a line motion of a point 'T'. Assume that the distances for the point on the path are measured from a reference point at regular intervals of time 'Δt'. We can estimate the velocity of 'T' at the i^{th} position 'V_i' as the arithmetic average of average velocities of adjacent segments of 'T_i':

$$V_i = \frac{\left(\frac{x_{i+1} - x_i}{\Delta t} + \frac{x_i - x_{i-1}}{\Delta t}\right)}{2} = \frac{x_{i+1} - x_{i-1}}{2\Delta t}$$

Eq. 1.5.5.5

Similarly, acceleration at 'T_i' can be estimated as the ratio of the difference in average velocities of adjacent segments of 'T_i' and the time interval 'Δt':

$$A_i = \frac{\frac{x_{i+1} - x_i}{\Delta t} - \frac{x_i - x_{i-1}}{\Delta t}}{\Delta t} = \frac{x_{i+1} - 2x_i + x_{i-1}}{(\Delta t)^2}$$

Eq. 1.5.5.6

Velocity and acceleration can be estimated at any position of the trajectory using the above formulae. This procedure can be used for motion analysis for which tabulating these results would be helpful.

For example, let us consider that a point traverses a path and name the consecutive positions as x_1, x_2, x_3, ..., x_{i-1}, x_i, x_{i+1}. The number of measurement is entered in the first column. The X-coordinate measured from an arbitrary point is entered in the second column. First difference values are calculated by subtracting values of corresponding pairs of adjacent numbers from the second column of positions as following:

$$\delta^1_{i-\frac{1}{2}} = x_i - x_{i-1}$$

Eq. 1.5.5.7

These values are entered in the third column. The subscript (i-1/2) in the above formula can be visualized as the rows of this column to be shifted by half a row with respect to the rows of the second column. Second differences are computed similarly by subtracting the two adjacent first difference values.

$$\delta_i^2 = \delta_{i+\frac{1}{2}}^1 - \delta_{i-\frac{1}{2}}^1 = (x_{i+1} - x_i) - (x_i - x_{i-1})$$

Eq. 1.5.5.8

Therefore,

$$\delta_i^2 = x_{i+1} - x_i + x_{i-1}$$

Eq. 1.5.5.9

It can be observed that first and second difference values can be used to calculate velocity and acceleration values. It is important to note that the above values are estimations. These estimations are fairly accurate if the displacement data is error free. In real applications, measurement data (displacement data) is never free of errors as discussed in the prior sections. Therefore, these inherent errors in measurement data accumulate into huge errors that are sometimes several times the original values of actual acceleration data. This problem is widely encountered while computing higher order derivatives using numerical methods. To tackle this problem, errors in measured displacement data can be reduced. J. Oderfeld proposed a method which is based on polynomial interpolation of measured displacement data and application of Stirling's interpolation formula for equidistant knots. Interpolation data can be differentiated to get the acceleration. In this proposed method, a cubic polynomial fit to seven points at a time with a 'marching point' scheme is applied.

Weights for adjustment are different for adjustment of first differences and second differences. They are computed using the 'marching point' technique and Stirling's formula. For example; there are eleven weights for adjusting second order data.

Table 1.5.5.1: Application of Adjustment Calculus

Position	S	δ'		δ''	
1	S_{i-6}				
		$\delta'_{i-11/2}$	$S_{i-5} - S_{i-6}$		
2	S_{i-5}			δ''_{i-5}	$\delta'_{i-9/2} - \delta'_{i-11/2}$
		$\delta'_{i-9/2}$	$S_{i-4} - S_{i-5}$		
3	S_{i-4}			δ''_{i-4}	$\delta'_{i-7/2} - \delta'_{i-9/2}$
		$\delta'_{i-7/2}$	$S_{i-3} - S_{i-4}$		
4	S_{i-3}			δ''_{i-3}	$\delta'_{i-5/2} - \delta'_{i-7/2}$
		$\delta'_{i-5/2}$	$S_{i-2} - S_{i-3}$		
5	S_{i-2}			δ''_{i-2}	$\delta'_{i-3/2} - \delta'_{i-5/2}$
		$\delta'_{i-3/2}$	$S_{i-1} - S_{i-2}$		
6	S_{i-1}			δ''_{i-1}	$\delta'_{i-1/2} - \delta'_{i-3/2}$
		$\delta'_{i-1/2}$	$S_i - S_{i-1}$		
7	S_i			δ''_i	$\delta'_{i+1/2} - \delta'_{i-1/2}$
		$\delta'_{i+1/2}$	$S_{i+1} - S_i$		
8	S_{i+1}			δ''_{i+1}	$\delta'_{i+3/2} - \delta'_{i+1/2}$
		$\delta'_{i+3/2}$	$S_{i+2} - S_{i+1}$		
9	S_{i+2}			δ''_{i+2}	$\delta'_{i+5/2} - \delta'_{i+3/2}$
		$\delta'_{i+5/2}$	$S_{i+3} - S_{i+2}$		
10	S_{i+3}			δ''_{i+3}	$\delta'_{i+7/2} - \delta'_{i+5/2}$
		$\delta'_{i+7/2}$	$S_{i+4} - S_{i+3}$		
11	S_{i+4}			δ''_{i+4}	$\delta'_{i+9/2} - \delta'_{i+7/2}$
		$\delta'_{i+9/2}$	$S_{i+5} - S_{i+4}$		
12	S_{i+5}			δ''_{i+5}	$\delta'_{i+11/2} - \delta'_{i+9/2}$
		$\delta'_{i+11/2}$	$S_{i+6} - S_{i+5}$		
13	S_{i+6}				

Therefore, to adjust the second difference at a position i, the product of δ^2_{i-5}, δ^2_{i-4}, δ^2_{i-3}, δ^2_{i-2}, δ^2_{i-1}, δ^2_i, δ^2_{i+1}, δ^2_{i+2}, δ^2_{i+3}, δ^2_{i+4}, δ^2_{i+5} and corresponding weights -0.0025, -0.0025, 0.015, 0.13, 0.25, 1, 0.25, 0.13, 0.015, -0.0025, -0.0025 respectively are added. The final adjusted value is the adjusted second difference $\delta_a{}^2{}_i$ [Table 1.5.5.1].

Therefore,

$$\delta^2_{a\,i} = (-0.0025) * \delta^2_{i-5} + (-0.0025) * \delta^2_{i-4} + (0.015) * \delta^2_{i-3} + (0.13) * \delta^2_{i-2} + (0.25) * \delta^2_{i-1} + (0.31) * \delta^2_{i} + (0.25) * \delta^2_{i+1} + (0.13) * \delta^2_{i+2} + (0.15) * \delta^2_{i+3} + (-0.0025) * \delta^2_{i+4} + (-0.0025) * \delta^2_{i+5}$$

Eq. 1.5.5.10

Similarly, the adjusted first difference at position 'i-1/2' can be calculated by adding the product of $\delta^1_{i-5/2}$, $\delta^1_{i-3/2}$, $\delta^1_{i-1/2}$, $\delta^1_{i+1/2}$, $\delta^1_{i+3/2}$, $\delta^1_{i+5/2}$ and weights 0.016667, -0.13333, 0.616667, 0.616667, -0.13333, 0.016667 respectively.

$$\delta^1_{a\,i-\frac{1}{2}} = (0.016667) * \delta^1_{i-\frac{5}{2}} + (-0.13333) * \delta^1_{i-\frac{3}{2}} + (0.616667) * \delta^1_{i-\frac{1}{2}} + (0.616667) * \delta^1_{i+\frac{1}{2}} + (-0.13333) * \delta^1_{i+\frac{3}{2}} + (0.016667) * \delta^1_{i+\frac{5}{2}}$$

Eq. 1.5.5.11

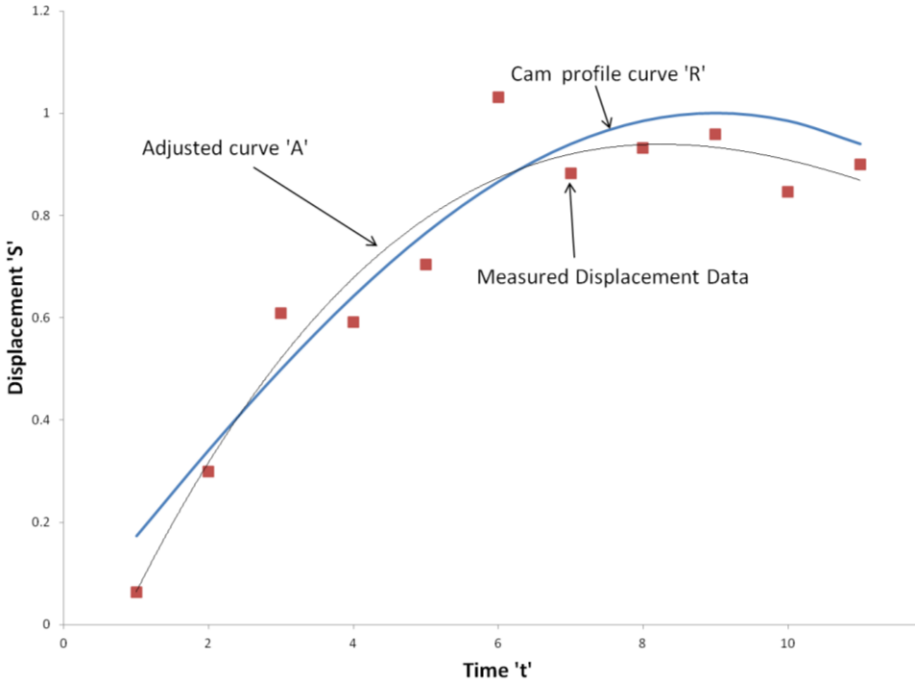

Figure 1.5.5.1: Theoretical Curve and Adjusted Curve

A numerical example is presented for calculation of adjusted second differences in Table 1.5.5.2. This procedure can be applied for calculation of velocities and accelerations. Adjusted first difference values can be divided by 'Δt' to get the value of adjusted velocity and adjusted second difference values can be divided by 'Δt^2' to obtain adjusted acceleration values.

Table 1.5.5.2: Numerical Example for Application of Adjustment Calculus

Position	S	δ'	δ''	Weights	δa"
1	0.000135				
		-0.00093			
2	0.001061		0.001534	-0.0025	-3.83401E-06
		-0.00246			
3	0.003521		0.002223	-0.0025	-5.5586E-06
		-0.00468			
4	0.008204		0.002862	0.015	4.29309E-05
		-0.00755			
5	0.01575		0.003451	0.13	0.000448589
		-0.011			
6	0.026746		0.003991	0.25	0.000997636
		-0.01499			
7	0.041732		0.004483	0.31	0.001389682
		-0.01947			
8	0.061202		0.004929	0.25	0.001232203
		-0.0244			
9	0.0856		0.00533	0.13	0.000692856
		-0.02973			
10	0.115328		0.005687	0.015	8.52993E-05
		-0.03541			
11	0.150742		-0.14474	-0.0025	0.000361853
		0.109327			
12	0.041415		0.115601	-0.0025	-0.000289001
		-0.00627			
13	0.047689				

1.6 Objective of this work:

The adjustment calculus technique is a lesser known technique to engineers but offers a promise for applications in cam-follower systems for quality control specifically

in estimation of velocity and acceleration data. Adjustment calculus will be studied in this work. Weights for adjusted acceleration calculation have already been derived. Weights for adjusted velocity determination will be derived using a cubic polynomial fit and the Symmetric Stirling interpolation formula. A procedure for application of this method for cam-follower systems will be formulated.

The effect of step size on the accuracy of estimated velocity and acceleration data during application of this procedure will be studied on various available cam profiles. The effect of location of dwell within the cam profile on optimum step selection will also be investigated.

2. DERIVATION OF WEIGHTS FOR VELOCITY

2.1 Weights for velocity:

As discussed earlier, Adjustment calculus is based on fitting a polynomial curve to discrete data measured at regular intervals of time and using the concept of a 'marching point' [19].

Let us assume a point 'P' traversing a path with 'N' displacements measured without errors at equivalent intervals of time 'h' shown as '♦' in Fig 2.1.1. When instruments are used to measure the displacements, errors are induced. Therefore, measured values that are denoted with '*' in Fig 2.1.1 deviate from actual values slightly. It is required to determine velocity and acceleration of the point traversing the path from the measured data as accurately as possible.

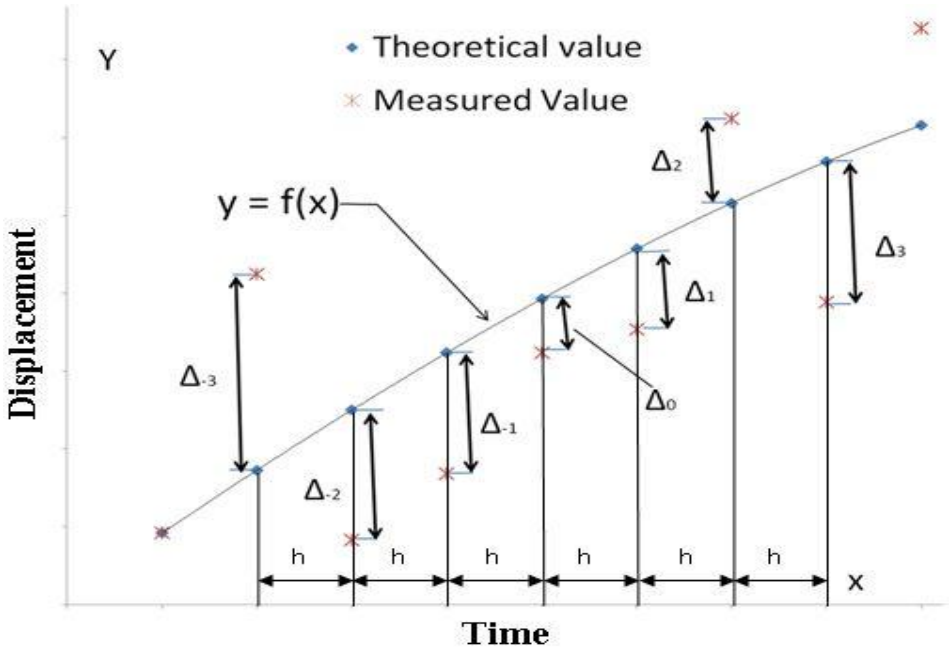

Figure 2.1.1: Displacement vs time plot – error functions

Out of these N points, seven chronologically consecutive points are selected initially. The fourth point is identified as 'i^{th}' point. Three points on either side are thus selected. The origin of the coordinate system is moved such that the time corresponding to the i^{th} point is zero. A cubic polynomial is fitted to approximate these seven consecutive displacements f_{i-3}, f_{i-2}, f_{i-1}, f_i, f_{i+1}, f_{i+2}, f_{i+3}:

$$y = C_0 + C_1 t + C_2 t^2 + C_3 t^3$$

Eq. 2.1.1

It needs to be observed here that any polynomial of order 'k' < N-1 can be used here. Selection of the third order polynomial is arbitrary and has the advantage of being the lowest order polynomial which can approximate a function with an inflection point.

Selection of a lower order polynomial simplifies the numerical calculations that are required.

Constants C_0 through C_3 from Eq. 2.1.1 need to be determined to solve for the value of the displacement 'y_i' with reduced error. At t=0, Eq. 2.1.1 reveals that only the value of 'C_0' needs to be determined. Fig 2.1.1 shows the deviations of the measured points from the cubic polynomial approximations. These deviations are defined as follows:

$$\Delta_{-3} = [f_{i-3} - x(-3h)]$$

Eq. 2.1.2

$$\Delta_{-2} = [f_{i-2} - x(-2h)]$$

Eq. 2.1.3

$$\Delta_{-1} = [f_{i-1} - x(-h)]$$

Eq. 2.1.4

$$\Delta_{0} = [f_{i} - x(0)]$$

Eq. 2.1.5

$$\Delta_{1} = [f_{i+1} - x(h)]$$

Eq. 2.1.6

$$\Delta_{2} = [f_{i+2} - x(2h)]$$

Eq. 2.1.7

$$\Delta_3 = [f_{i+3} - x(3h)]$$

Eq. 2.1.8

The coefficients of the cubic polynomial can be determined by minimizing the error function 'E':

$$E = \sum_{i=-3}^{3} (\Delta_i)^2$$

Eq. 2.1.9

Minimizing E can be expressed in algebraic equations in the unknowns C_0, C_1, C_2 and C_3 as:

$$\frac{\partial E}{\partial C_0} = 0, \qquad \frac{\partial E}{\partial C_1} = 0, \qquad \frac{\partial E}{\partial C_2} = 0, \qquad \frac{\partial E}{\partial C_3} = 0$$

Eq. 2.1.10

Maple software was used to solve the above equations [appendix 1]. By solving Eq. 2.1.10 for C_0, we get:

$$C_0 = -\frac{2}{21}(f_{i-3} + f_{i+3}) + \frac{1}{7}(f_{i-2} + f_{i+2}) + \frac{2}{7}(f_{i-1} + f_{i+1}) + \frac{1}{3}f_i$$

Eq. 2.1.11

It has to be noted here that C_0 represents the adjusted value of displacement at t=0. Using Eq. 2.1.11 and moving the coordinate system from one point to another, adjusted values for all displacements can be determined. The finite difference method [16] can then be

used to estimate the velocity and acceleration for the chosen point. An interpolation formula is applied that can be differentiated for this purpose. Stirling's formula is used for this purpose. There are various forms of Stirling's formulae that are available in literature [20][21][22]. Symmetric Stirling formula with equidistant knots [22], which has the most concise form, is the interpolation technique that is employed here. This formula is given as:

$$y(x) = y_0 + u\left(w_1 + \frac{u}{2}\left(\delta^2 y_0 + c_2\left(w_3 + \frac{u}{4}\left(\delta^4 y_0 + c_4(\delta^6 y_0 + \cdots)\right)\right)\right)\right) + R_r$$

Eq. 2.1.12

where

$$u = \frac{x}{h}, \qquad c_2 = \frac{u^2 - 1}{3u}, \qquad c_4 = \frac{u^2 - 2^2}{5u}, \qquad c_6 = \frac{u^2 - 3^2}{7u}, \qquad c_{2k} = \frac{u^2 - k^2}{(2k+1)u},$$

$$w_1 = \frac{1}{2}\left(\delta y_{-\frac{1}{2}} + \delta y_{\frac{1}{2}}\right), w_3 = \frac{1}{2}\left(\delta^3 y_{-\frac{1}{2}} + \delta^3 y_{\frac{1}{2}}\right), w_{2k-1} = \frac{1}{2}\left(\delta^{2k-1} y_{-\frac{1}{2}} + \delta^{2k-1} y_{\frac{1}{2}}\right),$$

$$\delta^{2k-1} y_{-\frac{1}{2}} = \delta^{2k-2} y_0 - \delta^{2k-2} y_{-1}, \qquad \delta^{2k-1} y_{\frac{1}{2}} = \delta^{2k-2} y_1 - \delta^{2k-2} y_0$$

$$\delta^n y_0 = \sum_{r=0}^{n} (-1)^r \binom{n}{r} y_{\frac{n}{2}-r}, \quad \delta^n y_j = \sum_{r=0}^{n} (-1)^r \binom{n}{r} y_{j+\frac{n}{2}-r},$$

R_r is the remainder and its value can be determined from:

$$|R_r| \leq \left|\frac{(u + .5r)^r}{r!} h^r [max D^r f(\eta)]\right|$$

Eq. 2.1.13

where

$$\eta = rh$$

Table 2.1.1: Central differences for discrete values

x_{-2}	y_{-2}				
		$\delta y_{-3/2}$			
x_{-1}	y_{-1}		$\delta^2 y_{-1}$		
		$\delta y_{-1/2}$		$\delta^3 y_{-1/2}$	
x_0	y_0		$\delta^2 y_0$		$\delta^4 y_0$
		$\delta y_{1/2}$		$\delta^3 y_{1/2}$	
x_1	y_1		$\delta^2 y_1$		
		$\delta y_{3/2}$			
x_2	y_2				

By adjustment, an expression for 'y_i' is obtained as:

$$y_i = C_0 = -\frac{2}{21}(f_{i-3} + f_{i+3}) + \frac{1}{7}(f_{i-2} + f_{i+2}) + \frac{2}{7}(f_{i-1} + f_{i+1}) + \frac{1}{3}f_i$$

Eq. 2.1.14

By substituting Eq. 2.1.14 in Eq. 2.1.12, 'y(x)' is obtained in a form that can be differentiated with respect to time 'x' to obtain the estimates of velocity at the knot positions.

$$v(x) = \frac{\partial y(x)}{\partial x}$$

Eq. 2.1.15

Here 'v(x)' is the adjusted first difference. After differentiation, values of the velocity is calculated at 'x=0' to determine the value of the adjusted first difference of the point that we are interested in. Therefore, after simplification the adjusted first difference is given as:

$$v_0 = \frac{1}{60}\left(\frac{30\delta y_{-\frac{1}{2}} + 30d\delta - 5\delta^3 y_{-\frac{1}{2}} - 5\delta^3 y_{\frac{1}{2}} + \delta^5 y_{-\frac{1}{2}} + \delta^5 y_{\frac{1}{2}}}{h}\right)$$

Eq. 2.1.16

Simplifying further we get an expression for 'v_0' purely in terms of first differences as:

$$v_0 = \frac{1}{60}\left(\frac{37\delta y_{-\frac{1}{2}} + 37\delta y_{\frac{1}{2}} - 8\delta y_{-\frac{3}{2}} - 8\delta y_{\frac{3}{2}} + \delta y_{-\frac{5}{2}} + \delta y_{\frac{5}{2}}}{h}\right)$$

Eq. 2.1.17

Thus the weights for velocity are 0.01667, -0.1333, 0.61667, 0.61667, -0.1333 and 0.01667 respectively. Adjusted velocity can be achieved by multiplying these weights with the corresponding first differences and dividing by the time step 'h'.

$$v_0 = \left[0.01667 * \delta y_{-\frac{5}{2}} - 0.1333 * \delta y_{-\frac{3}{2}} + 0.61667 * \delta y_{-\frac{1}{2}} + 0.61667 * \delta y_{\frac{1}{2}} - 0.1333 * \delta y_{\frac{3}{2}} + 0.01667 * \delta y_{\frac{5}{2}}\right] / h$$

Eq. 2.1.18

2.2 Weights for acceleration:

Weights for acceleration were derived by Dr. J. Oderfeld [19] and are given as follows:

$$a_0 = [0.31 * \delta^2 y_0 + 0.25 * (\delta^2 y_{-1} + \delta^2 y_1) + 0.135 * (\delta^2 y_{-2} + \delta^2 y_2) - 0.025 * (\delta^2 y_{-3} + \delta^2 y_3) - 0.025 * (\delta^2 y_{-4} + \delta^2 y_4) + 0.015 * (\delta^2 y_{-5} + \delta^2 y_5)\ ]/h^2$$

Eq. 2.2.1

3. APPLICATION OF ADJUSTMENT CALCULUS

3.1 Cams with Basic Curves and their Motion Characteristics

A set of different basic curves were used to define the cam profiles in this work to duplicate commercial cams. These curves are given in Chen [16]. These curves have been modified in a few cases. All the curves that were used and their motion characteristics are as follows:

3.1.1 Cycloidal Cam:

The profile of a cycloidal cam with cam length ‘L’ was considered. The profile of the cams can be divided into segments. These segments can be any combination of rise, fall and dwell. These combinations are meticulously selected to maintain continuity in the motion characteristics, i.e., to avoid excessive jerk or first time derivative of acceleration.

Span of each segment is ‘β’. Displacement of the cam is defined as the distance traversed by the follower from the cam. The rise part of the cam profile is given as:

$$S = L(\frac{\theta}{\beta} - \frac{1}{2\pi}\sin 2\pi\frac{\theta}{\beta})$$

Eq. 3.1.1.1

where

θ = Angle from initial point

L = Length of the cam

Theoretical velocity for the rise portion is calculated using the formula

$$V_{th} = \frac{\omega L}{\beta}(1 - \cos 2\pi\frac{\theta}{\beta})$$

Eq. 3.1.1.2

where

$\omega = \dot{\theta}$ – Angular Velocity

Theoretical acceleration for rise portion is calculated using the formula

$$A_{th} = \frac{2\pi L\omega^2}{\beta^2}(\sin 2\pi\frac{\theta}{\beta})$$

Eq. 3.1.1.3

Similarly for the fall part of the cam profile, motion characteristics are given as follows:

$$S = L(1 - \frac{\theta}{\beta} + \frac{1}{2\pi}\sin 2\pi\frac{\theta}{\beta})$$

Eq. 3.1.1.4

Theoretical velocity for the fall portion is calculated using the formula

$$V_{th} = -\frac{\omega L}{\beta}(1 - \cos 2\pi\frac{\theta}{\beta})$$

Eq. 3.1.1.5

Theoretical acceleration for fall portion is calculated using the formula

$$A_{th} = -\frac{2\pi L\omega^2}{\beta^2}(\sin 2\pi\frac{\theta}{\beta})$$

Eq. 3.1.1.6

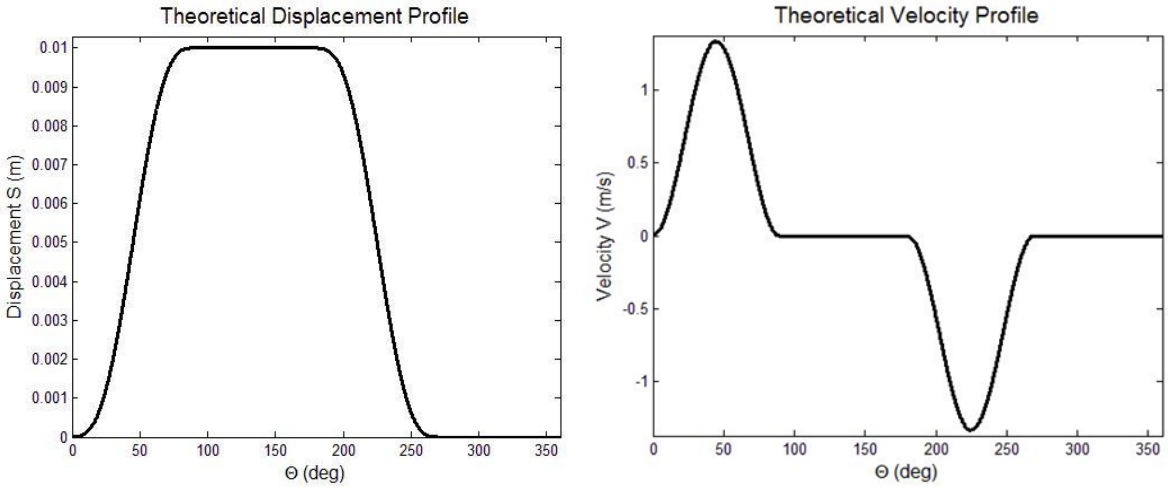

Figure 3.1.1.1: Theoretical displacement and velocity profiles of cycloidal cam

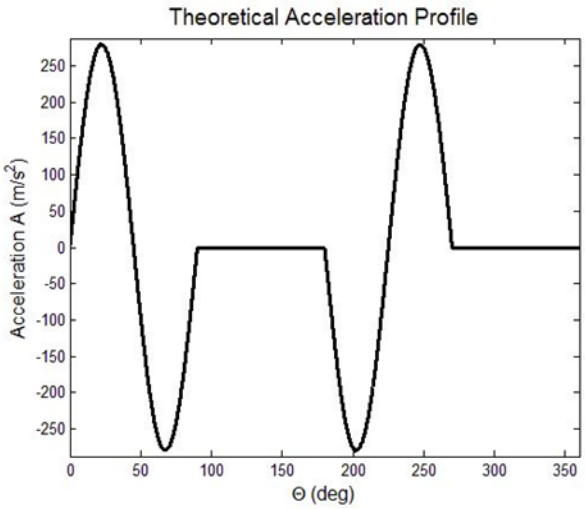

Figure 3.1.1.2: Theoretical acceleration profile for cycloidal cam

3.1.2 Harmonic Cam:

The profile of a harmonic cam with cam length 'L' was considered. The profile is comprised of two segments, rise and fall. The rise part of the cam profile is given as

$$S = \frac{L}{2}(1 - \cos\pi\frac{\theta}{\beta})$$

Eq. 3.1.2.1

Theoretical velocity for the rise portion is calculated using the formula

$$V_{th} = \frac{\omega\pi L}{2\beta}(\sin\pi\frac{\theta}{\beta})$$

Eq. 3.1.2.2

Theoretical acceleration for rise portion is calculated using the formula

$$A_{th} = \frac{\pi^2 L\omega^2}{2\beta^2}(\cos\pi\frac{\theta}{\beta})$$

Eq. 3.1.2.3

Similarly for the fall part of the cam profile, motion characteristics are given as follows

$$S = \frac{L}{2}(1 + \cos\pi\frac{\theta}{\beta})$$

Eq. 3.1.2.4

Theoretical velocity for the fall portion is calculated using the formula

$$V_{th} = \frac{\omega\pi L}{2\beta}(sin\,\pi\frac{\theta}{\beta})$$

Eq. 3.1.2.5

Theoretical acceleration for fall portion is calculated using the formula

$$A_{th} = -\frac{2\pi L\omega^2}{\beta^2}(\sin 2\pi\frac{\theta}{\beta})$$

Eq. 3.1.2.6

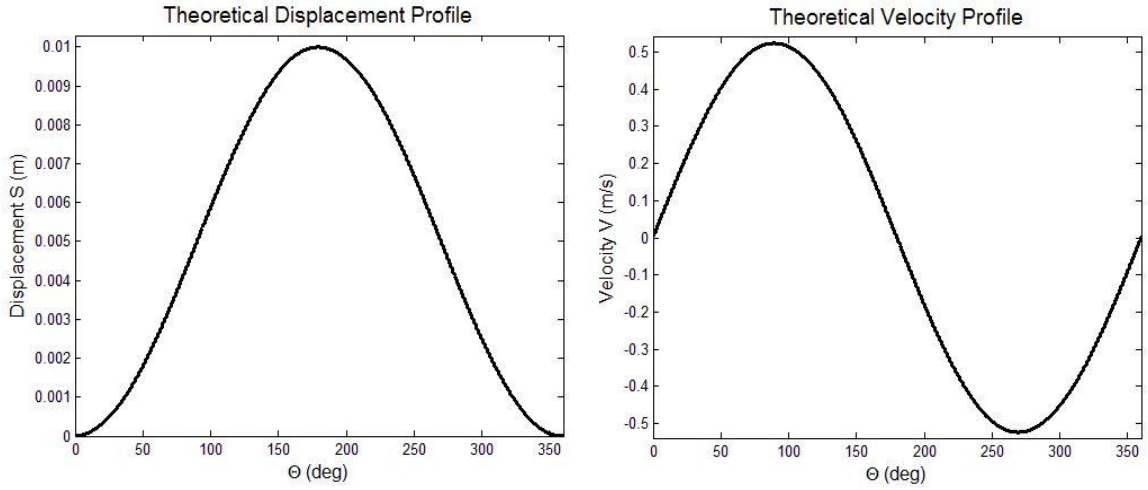

Figure 3.1.2.1: Theoretical displacement and velocity profiles of harmonic cam

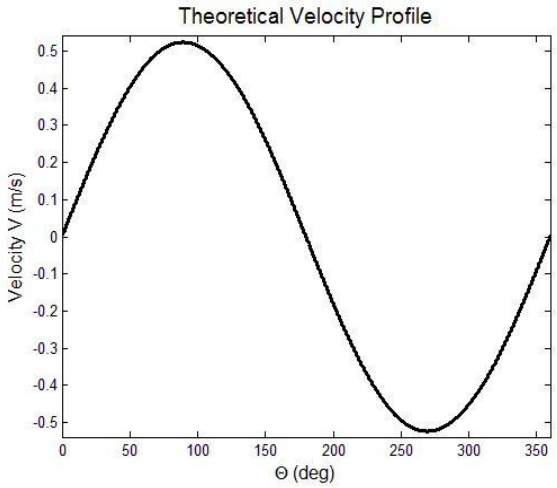

Figure 3.1.2.2: Theoretical acceleration profile for harmonic cam

3.1.3 3-4-5 Polynomial Cam:

A 3-4-5 polynomial cam of cam length 'L' was considered. The rise part of the cam profile is given as

$$S = L(0.62471\theta^5 - 2.46384\theta^4 + 2.58012\theta^3)$$

Eq. 3.1.3.1

Theoretical velocity for the rise portion is calculated using the formula

$$V_{th} = \omega L(3.13705\theta^4 - 9.85536\theta^3 + 7.74036\theta^2)$$

Eq. 3.1.3.2

Theoretical acceleration for rise portion is calculated using the formula

$$A_{th} = \omega L^2(12.5482\theta^3 - 29.56608\theta^2 + 15.48072\theta)$$

Eq. 3.1.3.3

Similarly for the fall part of the cam profile, motion characteristics are given as follows

$$S = L(1 - 0.62471\theta^5 + 2.46384\theta^4 - 2.58012\theta^3)$$

Eq. 3.1.3.4

Theoretical velocity for the fall portion is calculated using the formula

$$V_{th} = -\omega L(3.13705\theta^4 - 9.85536\theta^3 + 7.74036\theta^2)$$

Eq. 3.1.3.5

Theoretical acceleration for fall portion is calculated using the formula

$$A_{th} = -\omega L^2(12.5482\theta^3 - 29.56608\theta^2 + 15.48072\theta)$$

Eq. 3.1.3.6

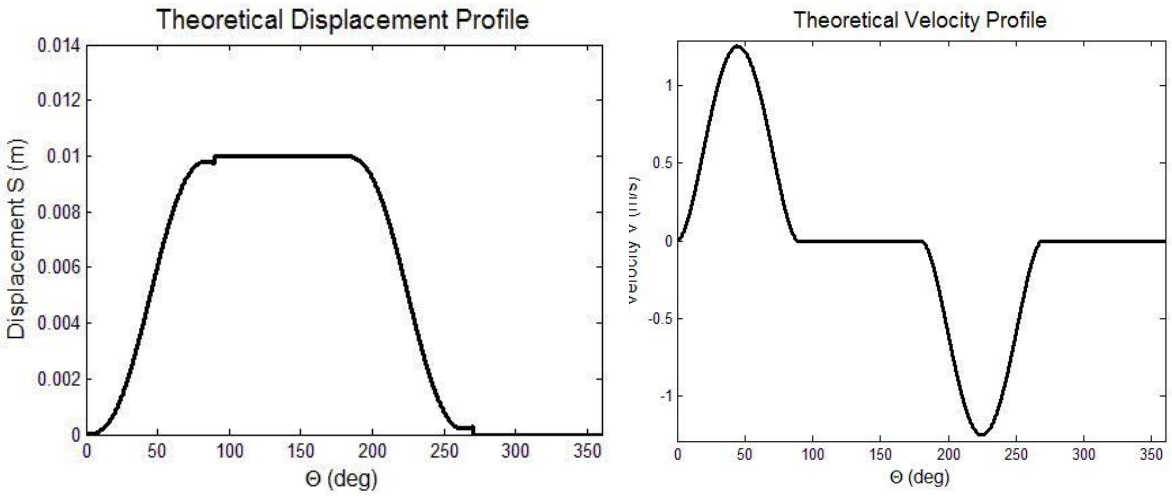

Figure 3.1.3.1: Theoretical displacement and velocity profiles of 3-4-5 polynomial cam

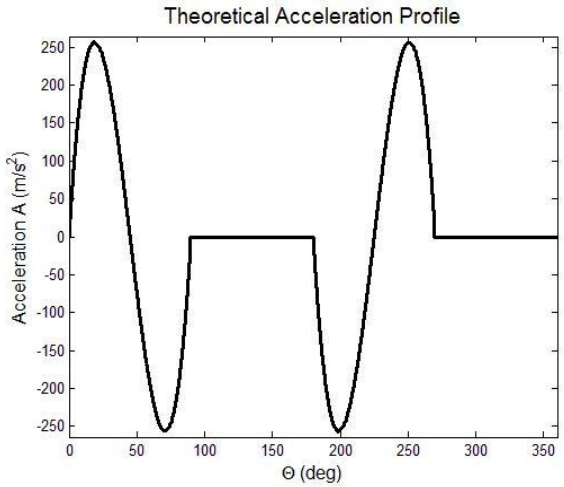

Figure 3.1.3.2: Theoretical acceleration profile for 3-4-5 polynomial cam

3.1.4 Polynomial Cam P1P2:

A polynomial cam of order 8 of cam length 'L' was considered. The rise part of the cam profile is given as

$$S = L(6.09755(\frac{\theta}{\beta})^3 - 20.7804(\frac{\theta}{\beta})^5 + 26.73155(\frac{\theta}{\beta})^6 - 13.60965(\frac{\theta}{\beta})^7 + 2.56095(\frac{\theta}{\beta})^8)$$

Eq. 3.1.4.1

Theoretical velocity for the rise portion is calculated using the formula

$$V_{th} = \frac{\omega L}{\beta}(18.29265\left(\frac{\theta}{\beta}\right)^2 - 103.902\left(\frac{\theta}{\beta}\right)^4 + 160.3893\left(\frac{\theta}{\beta}\right)^5 - 95.26755\left(\frac{\theta}{\beta}\right)^6 + 20.4876(\frac{\theta}{\beta})^7)$$

Eq. 3.1.4.2

Theoretical acceleration for rise portion is calculated using the formula

$$A_{th} = \frac{\omega L^2}{\beta}(36.5853\frac{\theta}{\beta} - 415.608\left(\frac{\theta}{\beta}\right)^3 + 801.9465\left(\frac{\theta}{\beta}\right)^4 - 571.6053\left(\frac{\theta}{\beta}\right)^5 + 143.4132(\frac{\theta}{\beta})^6)$$

Eq. 3.1.4.3

Similarly for the fall part of the cam profile, motion characteristics are given as follows

$$S = L(1 - 2.63415\left(\frac{\theta}{\beta}\right)^2 + 2.78055\left(\frac{\theta}{\beta}\right)^5 + 3.1706\left(\frac{\theta}{\beta}\right)^6 - 6.87795\left(\frac{\theta}{\beta}\right)^7 + 2.56095(\frac{\theta}{\beta})^8)$$

Eq. 3.1.4.4

Theoretical velocity for the fall portion is calculated using the formula

$$V_{th} = \frac{\omega L}{\beta}(-5.2683\frac{\theta}{\beta} + 13.90275\left(\frac{\theta}{\beta}\right)^4 + 19.0236\left(\frac{\theta}{\beta}\right)^5 - 43.14565\left(\frac{\theta}{\beta}\right)^6 + 20.4876(\frac{\theta}{\beta})^7)$$

Eq. 3.1.4.5

Theoretical acceleration for fall portion is calculated using the formula

$$A_{th} = \frac{\omega L^2}{\beta}(-5.2683 + 55.611\left(\frac{\theta}{\beta}\right)^3 + 95.118\left(\frac{\theta}{\beta}\right)^4 - 288.8739\left(\frac{\theta}{\beta}\right)^5 + 143.4132(\frac{\theta}{\beta})^6)$$

Eq. 3.1.4.6

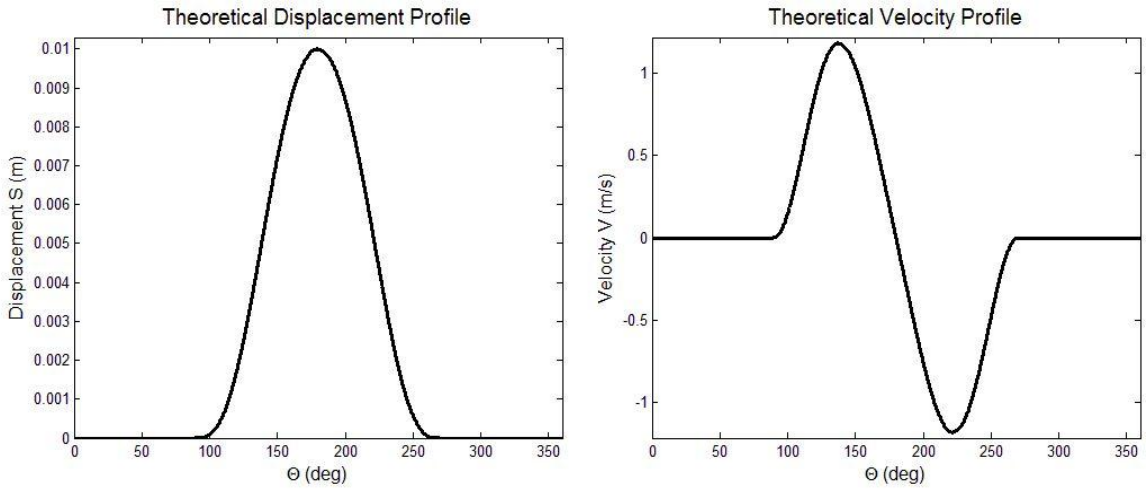

Figure 3.1.4.1: Theoretical displacement and velocity profiles of polynomial cam P1P2

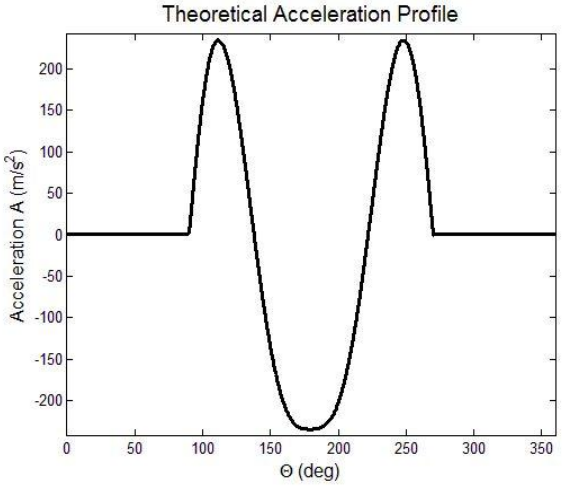

Figure 3.1.4.2: Theoretical acceleration profile of polynomial cam P1P2

3.1.5 4-5-6-7 Polynomial Cam:

A 4-5-6-7 Polynomial cam of order 8 of cam length 'L' was considered. The rise part of the cam profile is given as

$$S = L(5.7489\theta^4 - 8.784\theta^5 + 4.6599\theta^6 - 0.847599\theta^7)$$

Eq. 3.1.5.1

Theoretical velocity for the rise portion is calculated using the formula

$$V_{th} = \omega L(22.9956\theta^3 - 43.92\theta^4 + 27.9594\theta^5 - 5.933193\theta^6)$$

Eq. 3.1.5.2

Theoretical acceleration for rise portion is calculated using the formula

$$A_{th} = \omega^2 L(68.9868\theta^2 - 175.68\theta^3 + 139.797\theta^4 - 35.599158\theta^5)$$

Eq. 3.1.5.3

Similarly for the fall part of the cam profile, motion characteristics are given as follows

$$S = L(1 - 5.7489\theta^4 + 8.784\theta^5 - 4.6599\theta^6 + 0.847599\theta^7)$$

Eq. 3.1.5.4

Theoretical velocity for the fall portion is calculated using the formula

$$V_{th} = -\omega L(22.9956\theta^3 - 43.92\theta^4 + 27.9594\theta^5 - 5.933193\theta^6)$$

Eq. 3.1.5.5

Theoretical acceleration for fall portion is calculated using the formula

$$A_{th} = -\omega^2 L(68.9868\theta^2 - 175.68\theta^3 + 139.797\theta^4 - 35.599158\theta^5)$$

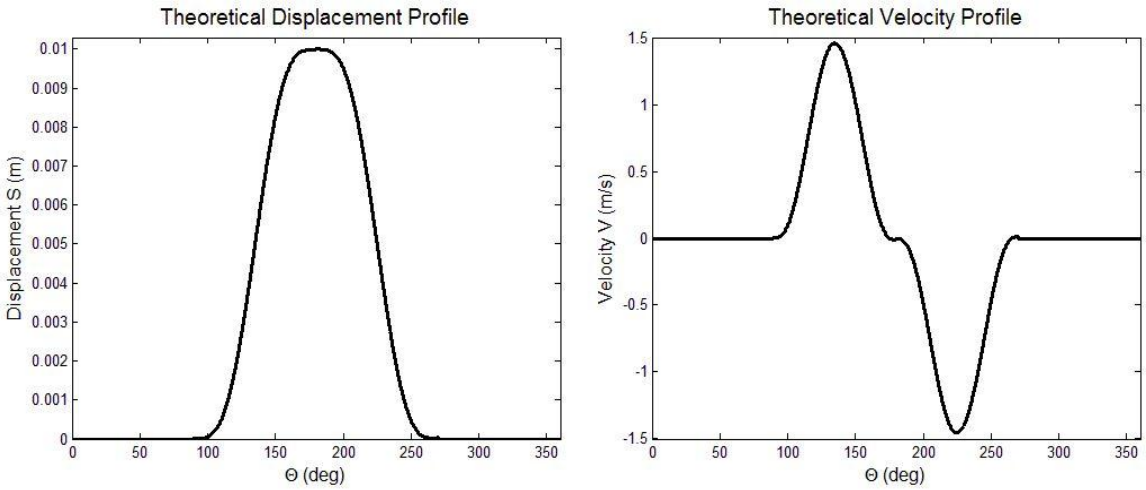

Eq. 3.1.5.6

Figure 3.1.5.1: Theoretical displacement and velocity profiles of 4-5-6-7 polynomial cam

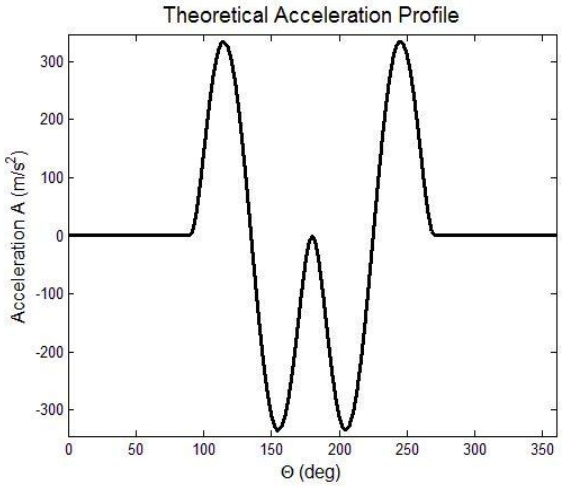

Figure 3.1.5.2: Theoretical acceleration profile of 4-5-6-7 polynomial cam

3.1.6 Modified Trapezoidal Cam:

A modified trapezoidal cam of length 'L' is selected. This cam can be interpreted as a combination of different curves. Therefore its motion characteristics will be written separately for each section. 'γ' is used to represent the ratio of 'θ' and 'β'. Rise part of the cam profile is given as;

For $0 \leq \gamma \leq 1/8$

The displacement profile is given as

$$S = 0.09724612L(4\gamma - \frac{1}{\pi} sin4\pi\gamma)$$

Eq. 3.1.6.1

Theoretical velocity of this portion of rise is given as

$$V_{th} = 0.3889845 \frac{\omega L}{\beta}(1 - cos4\pi\gamma)$$

Eq. 3.1.6.2

Theoretical acceleration of this portion of rise is given as

$$A_{th} = 4.888124 \frac{\omega^2 L}{\beta^2}(sin4\pi\gamma)$$

Eq. 3.1.6.3

For $1/8 \leq \gamma \leq 3/8$

The displacement profile is given as

$$S = L(2.44406184\gamma^2 - 0.22203097\gamma + 0.00723407)$$

Eq. 3.1.6.4

Theoretical velocity of this portion of rise is given as

$$V_{th} = \frac{\omega L}{\beta}(4.888124\gamma - 0.222031)$$

Eq. 3.1.6.5

Theoretical acceleration of this portion of rise is given as

$$A_{th} = 4.888124\ \frac{\omega^2 L}{\beta^2}$$

Eq. 3.1.6.6

For $3/8 \leq \gamma \leq 1/2$

The displacement profile is given as;

$$S = L(1.6110154\gamma - 0.0309544\sin(4\pi\gamma - \pi) - 0.3055077)$$

Eq. 3.1.6.7

Theoretical velocity of this portion of rise is given as

$$V_{th} = \frac{\omega L}{\beta}(1.6110154 - 0.3889845\cos(4\pi\gamma - \pi))$$

Eq. 3.1.6.8

Theoretical acceleration of this portion of rise is given as

$$A_{th} = 4.888124\ \frac{\omega^2 L}{\beta^2}(\sin(4\pi\gamma - \pi)$$

Eq. 3.1.6.9

For $1/2 \leq \gamma \leq 5/8$

The displacement profile is given as

$$S = L(1.6110154\gamma + 0.0309544\sin(4\pi\gamma - 2\pi) - 0.3055077)$$

Eq. 3.1.6.10

Theoretical velocity of this portion of rise is given as

$$V_{th} = \frac{\omega L}{\beta}(1.6110154 + 0.3889845\cos(4\pi\gamma - 2\pi))$$

Eq. 3.1.6.11

Theoretical acceleration of this portion of rise is given as

$$A_{th} = -4.888124\ \frac{\omega^2 L}{\beta^2}(\sin(4\pi\gamma - 2\pi)$$

Eq. 3.1.6.12

For $5/8 \leq \gamma \leq 7/8$

The displacement profile is given as

$$S = L(-2.44406184\gamma^2 + 4.6660917\gamma\ - 1.2292648)$$

Eq. 3.1.6.13

Theoretical velocity of this portion of rise is given as

$$V_{th} = \frac{\omega L}{\beta}(-4.888124\gamma + 4.6660917)$$

Eq. 3.1.6.14

Theoretical acceleration of this portion of rise is given as

$$A_{th} = -4.888124\ \frac{\omega^2 L}{\beta^2}$$

Eq. 3.1.6.15

For $7/8 \leq \gamma \leq 1$

The displacement profile is given as

$$S = L(0.6110154 + 0.0309544\sin(4\pi\gamma - 3\pi) + 0.3889845\gamma)$$

Eq. 3.1.6.16

Theoretical velocity of this portion of rise is given as

$$V_{th} = \frac{\omega L}{\beta}(0.3889845 + 0.3889845\cos(4\pi\gamma - 3\pi))$$

Eq. 3.1.6.17

Theoretical acceleration of this portion of rise is given as

$$A_{th} = -4.888124\ \frac{\omega^2 L}{\beta^2}(\sin(4\pi\gamma - 3\pi)$$

Eq. 3.1.6.18

Similarly the fall portion of the profile is given as

For $0 \leq \gamma \leq 1/8$

The displacement profile is given as

$$S = L(1 - 0.09724612\left(4\gamma - \frac{1}{\pi}sin4\pi\gamma\right))$$

Eq. 3.1.6.19

Theoretical velocity of this portion of fall is given as

$$V_{th} = -0.3889845\frac{\omega L}{\beta}(1 - cos4\pi\gamma)$$

Eq. 3.1.6.20

Theoretical acceleration of this portion of fall is given as

$$A_{th} = -4.888124\ \frac{\omega^2 L}{\beta^2}(sin4\pi\gamma)$$

Eq. 3.1.6.21

For $1/8 \leq \gamma \leq 3/8$

The displacement profile is given as

$$S = L(1 - 2.44406184\gamma^2 + 0.22203097\gamma - 0.00723407)$$

Eq. 3.1.6.22

Theoretical velocity of this portion of fall is given as

$$V_{th} = \frac{\omega L}{\beta}(-4.888124\gamma + 0.222031)$$

Eq. 3.1.6.23

Theoretical acceleration of this portion of fall is given as

$$A_{th} = -4.888124\ \frac{\omega^2 L}{\beta^2}$$

Eq. 3.1.6.24

For $3/8 \leq \gamma \leq 1/2$

The displacement profile is given as

$$S = L(1 - 1.6110154\gamma + 0.0309544\sin(4\pi\gamma - \pi) + 0.3055077)$$

Eq. 3.1.6.25

Theoretical velocity of this portion of fall is given as

$$V_{th} = \frac{\omega L}{\beta}(-1.6110154 + 0.3889845\cos(4\pi\gamma - \pi))$$

Eq. 3.1.6.26

Theoretical acceleration of this portion of fall is given as

$$A_{th} = -4.888124\ \frac{\omega^2 L}{\beta^2}(\sin(4\pi\gamma - \pi)$$

Eq. 3.1.6.27

For $1/2 \leq \gamma \leq 5/8$

The displacement profile is given as

$$S = L(1 - 1.6110154\gamma - 0.0309544\sin(4\pi\gamma - 2\pi) + 0.3055077)$$

Eq. 3.1.6.28

Theoretical velocity of this portion of fall is given as

$$V_{th} = \frac{\omega L}{\beta}(-1.6110154 - 0.3889845\cos(4\pi\gamma - 2\pi))$$

Eq. 3.1.6.29

Theoretical acceleration of this portion of fall is given as

$$A_{th} = 4.888124\ \frac{\omega^2 L}{\beta^2}(\sin(4\pi\gamma - 2\pi)$$

Eq. 3.1.6.30

For $5/8 \leq \gamma \leq 7/8$

The displacement profile is given as

$$S = L(2.44406184\gamma^2 - 4.6660917\gamma + 1.2292648)$$

Eq. 3.1.6.31

Theoretical velocity of this portion of fall is given as

$$V_{th} = \frac{\omega L}{\beta}(4.888124\gamma - 4.6660917)$$

Eq. 3.1.6.32

Theoretical acceleration of this portion of fall is given as

$$A_{th} = 4.888124\ \frac{\omega^2 L}{\beta^2}$$

Eq. 3.1.6.33

For $7/8 \leq \gamma \leq 1$;

The displacement profile is given as

$$S = L(1 - 0.6110154 - 0.0309544\sin(4\pi\gamma - 3\pi) - 0.3889845\gamma)$$

Eq. 3.1.6.34

Theoretical velocity of this portion of fall is given as

$$V_{th} = -\frac{\omega L}{\beta}(0.3889845 + 0.3889845\cos(4\pi\gamma - 3\pi))$$

Eq. 3.1.6.35

Theoretical acceleration of this portion of fall is given as

$$A_{th} = 4.888124\ \frac{\omega^2 L}{\beta^2}(\sin(4\pi\gamma - 3\pi)$$

Eq. 3.1.6.36

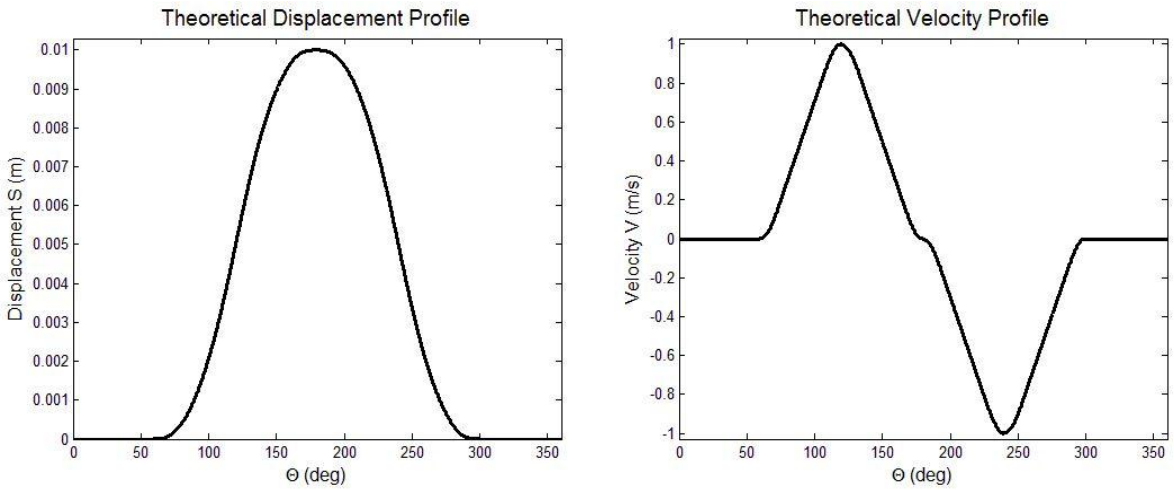

Figure 3.1.6.1: Theoretical displacement and velocity profiles of modified trapezoidal cam

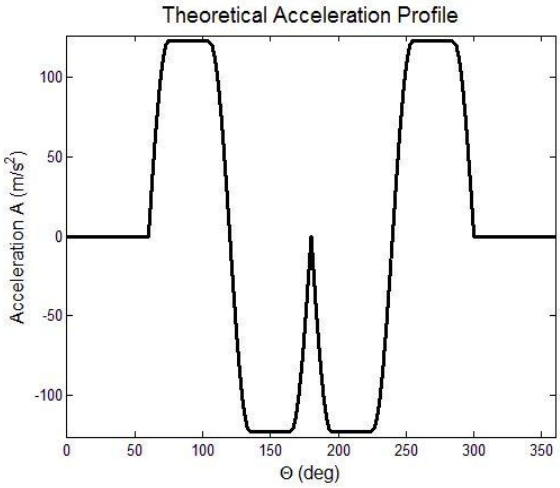

Figure 3.1.6.2: Theoretical acceleration profile of modified trapezoidal cam

3.1.7 Sine Cam:

The profile of a Sine cam with cam length ‘L’ was considered. The rise part of the cam profile is given as

$$S = Lsin\theta$$

Eq. 3.1.7.1

Theoretical velocity for the rise portion is calculated using the formula

$$V_{th} = \omega Lcos\theta$$

Eq. 3.1.7.2

Theoretical acceleration for rise portion is calculated using the formula

$$A_{th} = -\omega^2 Lsin\theta$$

Eq. 3.1.7.3

Similarly for the fall part of the cam profile, motion characteristics are given as follows

$$S = -Lsin\theta$$

Eq. 3.1.7.4

Theoretical velocity for the fall portion is calculated using the formula

$$V_{th} = -\omega Lcos\theta$$

Eq. 3.1.7.5

Theoretical acceleration for fall portion is calculated using the formula

$$A_{th} = \omega^2 L sin\theta$$

Eq. 3.1.7.6

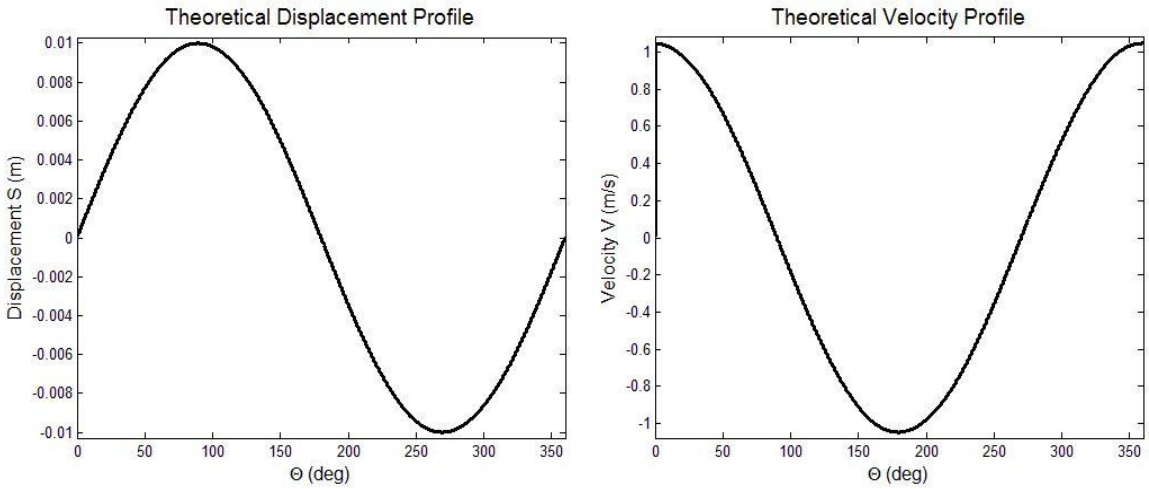

Figure 3.1.7.1: Theoretical displacement and velocity profiles of sine cam

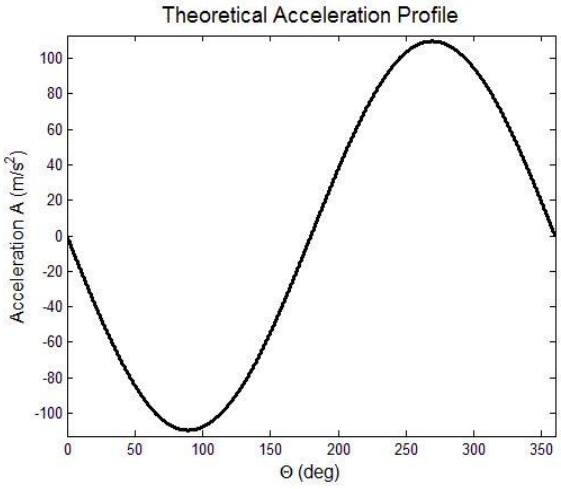

Figure 3.1.7.2: Theoretical acceleration profile of sine cam

3.2 Procedure to Analyze Effects of Errors

A cam is selected with prescribed rise and fall portions. Theoretical values of velocity and acceleration are calculated using section 3.1. A counter 'i' will be used to identify the point under consideration. First differences ($\delta_i^{'}$) are calculated by subtracting S_{i-1} from S_i. Second differences ($\delta_i^{''}$) are calculated by subtracting $\delta_{i-1}^{'}$ from $\delta_i^{'}$. Using the weights (six weights) for velocity, first adjusted differences ($\delta_{ai}^{'}$) are calculated using the formula

$$\delta_{a(i)}^{'} = \delta_{i-2}^{'} * w_0^v + \delta_{i-1}^{'} * w_1^v + \delta_i^{'} * w_2^v + \delta_{i+1}^{'} * w_3^v + \delta_{i+2}^{'} * w_4^v + \delta_{i+3}^{'} * w_5^v$$

Eq. 3.2.1

where

w_n^v – Weights for velocity $\vee$ n = 0 to 5

Using the weights for acceleration, second adjusted differences ($\delta_{ai}^{''}$) are calculated using the formula

$$\delta_{a(i)}^{''} = \delta_{i-5}^{''} * w_0^a + \delta_{i-4}^{''} * w_1^a + \delta_{i-3}^{''} * w_2^a + \delta_{i-2}^{''} * w_3^a + \delta_{i-1}^{''} * w_4^a + \delta_i^{''} * w_5^a + \delta_{i+1}^{''} * w_6^a + \delta_{i+2}^{''} * w_7^a + \delta_{i+3}^{''} * w_8^a + \delta_{i+4}^{''} * w_9^a + \delta_{i+5}^{''} * w_{10}^a$$

Eq. 3.2.2

where

w_n^a = Weights for acceleration $\vee$ n = 0 to 10

Unadjusted velocity is calculated using unadjusted first differences as follows

$$V_{unadj} = \frac{\delta'_{i+1} + \delta'_{i-1}}{2\Delta t}$$

Eq. 3.2.3

Adjusted velocity is calculated similarly but using adjusted first differences as follows

$$V_{adj} = \frac{\delta'_{a(i+1)} + \delta'_{a(i-1)}}{2\Delta t}$$

Eq. 3.2.4

Unadjusted acceleration is calculated using unadjusted second differences as follows

$$A_{unadj} = \frac{\delta''_{i}}{\Delta t^2}$$

Eq. 3.2.5

Adjusted acceleration is calculated using adjusted second differences as follows

$$A_{adj} = \frac{\delta''_{a(i)}}{\Delta t^2}$$

Eq. 3.2.6

These values are compared for analysis.

3.3 Determination of effect of errors using Monte Carlo method

The Monte Carlo method is a method which deals with implementation of computational algorithms which rely on repeated random sampling. The Monte Carlo method is specifically significant when there is randomness in input data. Monte Carlo

methods deal with simulating the phenomena by repeating a simulation many times by changing the random set of data each time [23]. As it has been discussed earlier that measurement errors contain random components, Monte Carlo simulations are used for this purpose.

'Matlab' software is used to implement these simulations. A 'Matlab' code is composed for each cam profile considered. The Step or the resolution of the simulation in terms of smallest angle increments considered is specified as a variable. The procedures given in sections 3.1 and 3.2 are applied to compute the values of theoretical, unadjusted and adjusted velocity and acceleration. The values of 'S' (profile) are tainted with normally distributed random errors with a specified standard deviation to account for random measurement errors. At the end of every iteration, deviations of unadjusted and adjusted values of velocity and acceleration from theoretical values are measured in the form of standard deviation calculated over the length of the profile. The means of these stored values is computed at the end of all iterations. Deviations at maximum values of theoretical velocity and acceleration are recorded over the iterations. The ratio of these deviations and maximum theoretical velocity and acceleration are calculated and are compared for analysis.

Application of adjustment calculus revealed that the selection of step size or the resolution of the displacement data influenced the resulting acceleration data. This study will focus on the effect of step size on adjustment calculus application.

4. MONTE CARLO METHOD AND STEP ANALYSIS

4.1 Effect of profile type on step size

The effect of different cam profiles on effective step size selection will be studied. Monte Carlo simulations will be implemented for cams with profiles discussed in section 3.1. Data will then be analyzed to suggest the best step size. Lift ‘L’ of all the cams that are considered is fixed at 0.01 m. Angular velocity is fixed at 104.71 rad/s corresponding to 1000 rpm. Magnitude of errors, i.e., standard deviation of random errors used to taint theoretical values, is 0.0000254 m in accordance with the allowable machining errors for commercial cams [2]. The number of iterations for each step is fixed at 1000. Tainted displacement data (with random errors) are referred to as ‘Measured’ displacement values.

4.1.1 Cycloidal cam:

A cycloidal cam with four segments Rise, Dwell, Fall and Dwell (RDFD), was selected for this study. The span of each segment 'β' is π/2.

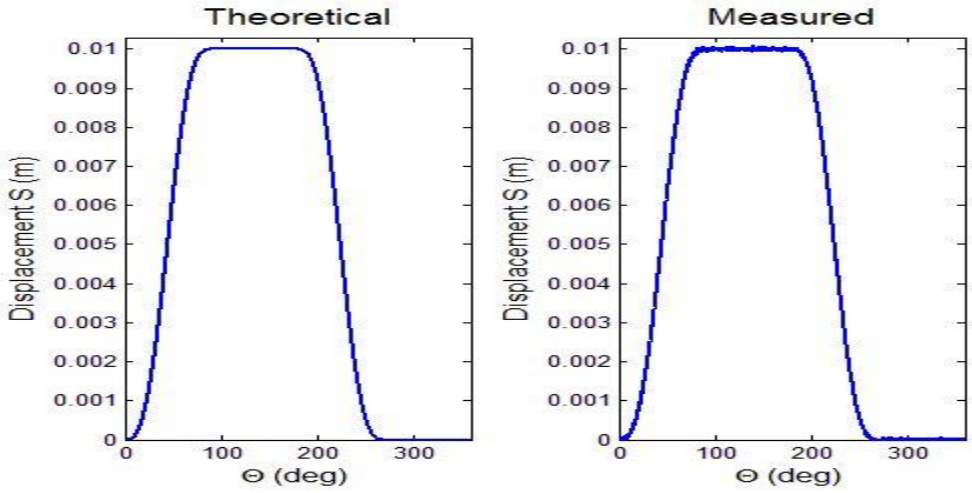

Figure 4.1.1.1: Theoretical and measured displacement profile of cycloidal cam

Measured profile is obtained by adding random errors that follow a normal distribution with expected value of zero and specified standard deviation, to theoretical profile. The effect of these small errors on velocity and acceleration values is shown later in this section by comparing theoretical, unadjusted and adjusted velocity and acceleration profiles, after adding random errors. Deviations of adjusted values of velocity from theoretical, before adding random errors, are systematic errors that are inherent to the system. Deviations in these values after adding random errors to displacement data yields error that contains both systematic and random errors. These errors are referred to as total error. The same nomenclature is extended to acceleration data. Effective step size analysis will be conducted.

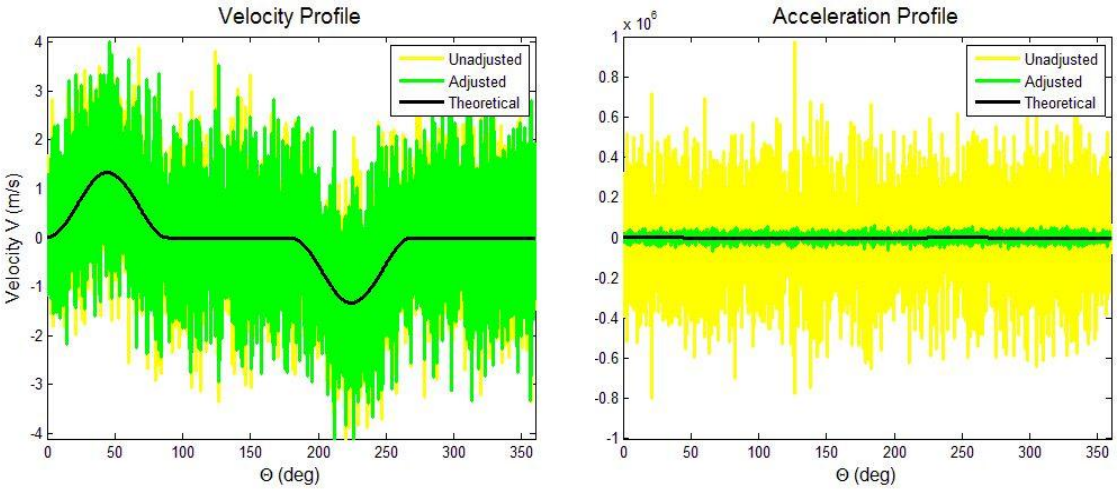

Figure 4.1.1.2: Comparison of theoretical, unadjusted and adjusted velocity and acceleration profiles of cycloidal cam at step size of 0.1˚

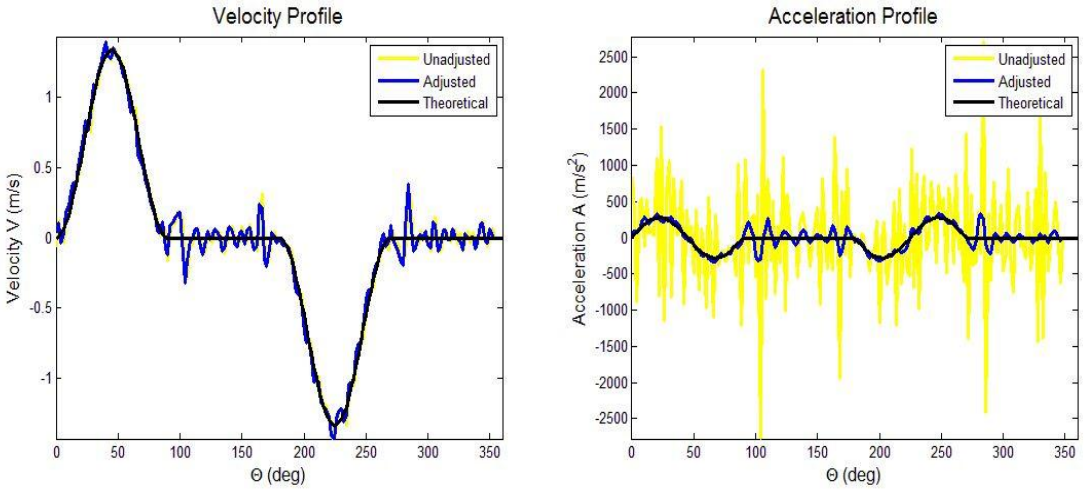

Figure 4.1.1.3: Comparison of theoretical, unadjusted and adjusted velocity and acceleration profiles of cycloidal cam at step size of 2˚

Theoretical, unadjusted and adjusted values of velocity and acceleration for a measured profile are shown in figures 4.1.1.2 and 4.1.1.3. It can be observed that a slight deviation in displacement profile can cause huge deviations in unadjusted and adjusted acceleration data. It can also be inferred that adjusted acceleration data is relatively more accurate than unadjusted acceleration data. Adjusted velocity and unadjusted velocity data are very close to each other. This phenomenon has been observed for all the cams that are considered. Therefore, comparison of only adjusted values of velocity and acceleration data, with theoretical values will be shown in the figures in later sections.

Table 4.1.1.1: Deviations at maximum velocity and acceleration of cycloidal cam at different step sizes

Step (degrees)	Percentage Error at Maximum Theoretical Values - Mean of n iterations			
	Velocity (m/s)		Acceleration (m/s^2)	
	Unadj	Adj	Unadj	Adj
0.05	1.32E+02	1.28E+02	2.64E+05	2.07E+04
0.1	6.40E+01	6.37E+01	6.62E+04	5.18E+03
0.25	2.52E+01	2.54E+01	9.99E+03	8.49E+02
0.5	1.31E+01	1.23E+01	2.59E+03	2.09E+02
0.75	8.42E+00	8.40E+00	1.18E+03	9.74E+01
1	6.47E+00	6.29E+00	6.38E+02	5.06E+01
2	3.14E+00	3.19E+00	1.56E+02	1.47E+01
3	2.18E+00	2.17E+00	6.86E+01	6.96E+00
5	1.51E+00	1.83E+00	2.56E+01	2.42E+00
6	1.67E+00	1.04E+00	1.69E+01	6.15E+00
9	3.19E+00	4.76E+00	9.09E+00	2.31E+01
10	3.82E+00	6.43E-01	7.47E+00	2.97E+01
15	8.68E+00	3.05E+01	8.91E+00	5.14E+01

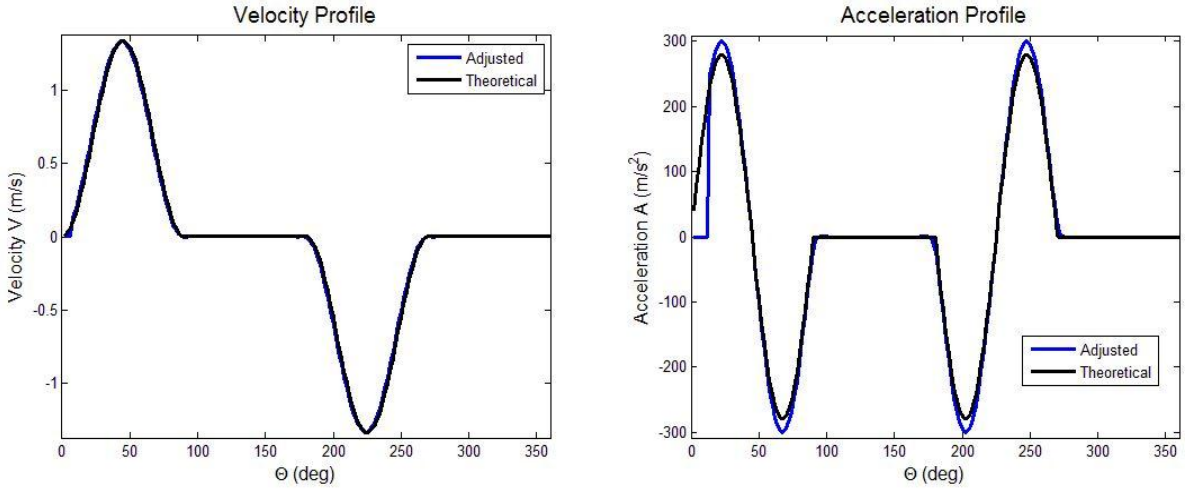

Figure 4.1.1.4: Velocity and acceleration profiles of cycloidal cam considering theoretical curve with a step size of 2˚

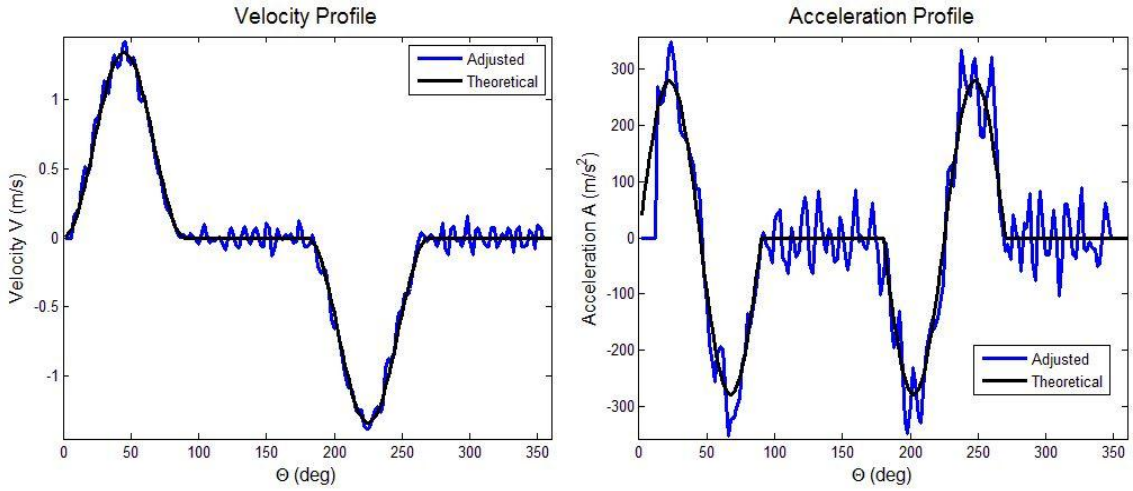

Figure 4.1.1.5: Velocity and acceleration profiles of cycloidal cam considering measured curve with a step size of 2˚

To further study the effect of random errors and step analysis, deviations of unadjusted and adjusted values from theoretical values are considered at peak values of velocity and acceleration (Table 4.1.1.1). The acceleration data is given importance over velocity data during analysis as cam manufacturers analyze the cams based on acceleration data. Table 4.1.1.2 reveals that deviation of adjusted acceleration from theoretical acceleration corresponding to the angle at maximum theoretical acceleration is lowest at a step size of 5˚. Therefore, this study suggests that selecting step size of 5˚ for a cycloidal cam with a RDFD profile at specified angular velocity and lift of cam will give relatively more efficient results. Maximum acceleration can be estimated with a percentage error of 2.42% from measured displacement data using adjustment calculus.

Figure 4.1.1.4 displays the systematic errors in velocity and acceleration due to the use of adjustment calculus. It can be observed that the systematic error at maximum velocity is hardly noticeable whereas the systematic error at maximum theoretical acceleration is visible.

Figure 4.1.1.5 displays the total errors in velocity and acceleration due to the use of adjustment calculus. In velocity and acceleration profiles, it can be observed that deviations of adjusted values are more at dwells. Since the designer is aware that the values of velocity and acceleration at dwells are zero, these deviations can be ignored.

4.1.2 Harmonic cam:

A harmonic cam with Rise, Fall and Rise (RFR) profile was selected. Span of each segment 'β' is π.

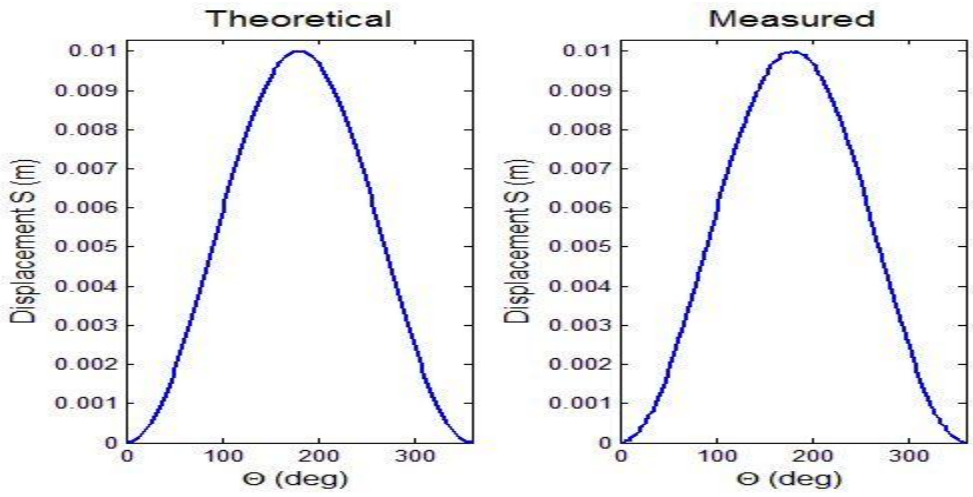

Figure 4.1.2.1: Theoretical and measured displacement profile of harmonic cam

Figure 4.1.2.1 shows the profile of harmonic cam before and after adding random errors. Table 4.1.2.1 reveals that deviation of adjusted acceleration from theoretical acceleration corresponding to the angle at maximum theoretical acceleration is lowest at a step size of 18˚. Therefore, this study suggests that selecting step size of 18˚ for a harmonic cam with a RFR profile at the specified angular velocity and lift of cam will give relatively more efficient results. Maximum acceleration can be estimated with a percentage error of 0.88% from measured displacement data using adjustment calculus. A smaller step can be considered to prevent loss of data due to the use of a higher step size.

Table 4.1.2.1: Deviations at maximum velocity and acceleration of harmonic cam at different step sizes

Step (degrees)	Percentage Error at maximum theoretical values - mean of n iterations			
	Velocity (m/s)		Acceleration (m/s^2)	
	Unadj	Adj	Unadj	Adj
0.05	3.26E+02	3.32E+02	1.32E+06	1.10E+05
0.1	1.65E+02	1.60E+02	3.21E+05	2.72E+04
0.25	6.22E+01	6.40E+01	5.28E+04	4.27E+03
0.5	3.38E+01	3.26E+01	1.36E+04	1.06E+03
0.75	2.18E+01	2.17E+01	5.76E+03	4.92E+02
1	1.64E+01	1.60E+01	3.29E+03	2.67E+02
2	8.07E+00	8.17E+00	8.25E+02	6.94E+01
3	5.47E+00	5.21E+00	3.64E+02	3.13E+01
5	3.26E+00	3.21E+00	1.30E+02	1.26E+01
6	2.80E+00	2.68E+00	9.20E+01	1.03E+01
9	1.82E+00	1.85E+00	4.04E+01	7.05E+00
10	1.69E+00	1.77E+00	3.17E+01	6.47E+00
15	1.47E+00	5.13E+00	1.45E+01	3.03E+00
18	1.80E+00	1.37E+01	9.59E+00	8.86E-01
20	2.16E+00	2.34E+01	8.09E+00	1.63E+00

Figure 4.1.2.2 displays the systematic errors in velocity and acceleration profile and Figure 4.1.2.3 displays the total errors. Truncations on the ends of the profiles are due to the 'Matlab' codes and should be ignored. An absence of dwell shows the efficiency of adjustment calculus in estimating the values of velocity and acceleration.

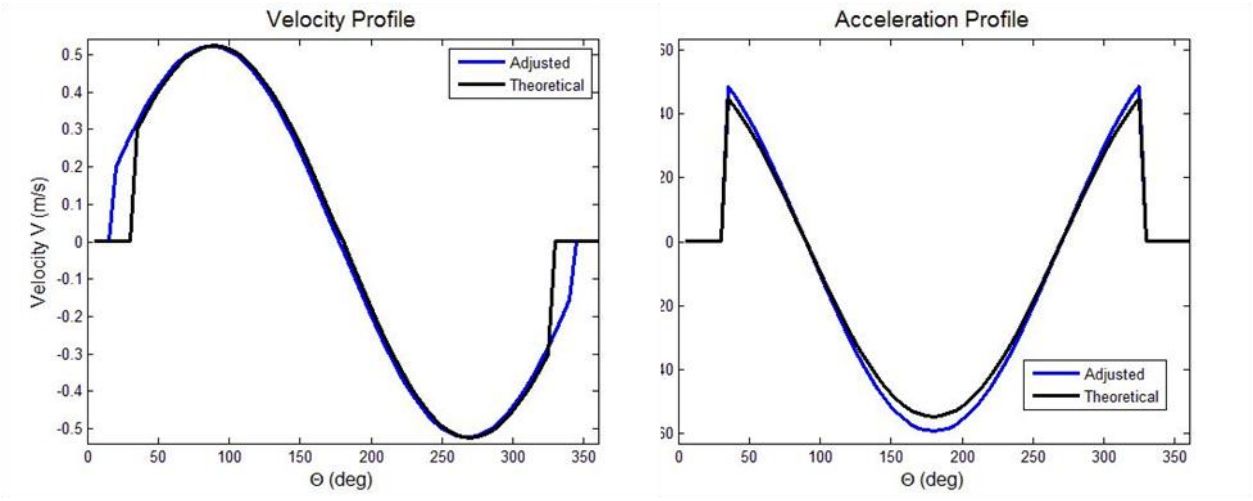

Figure 4.1.2.2: Velocity and acceleration profiles of harmonic cam considering theoretical curve with a step size of 5˚

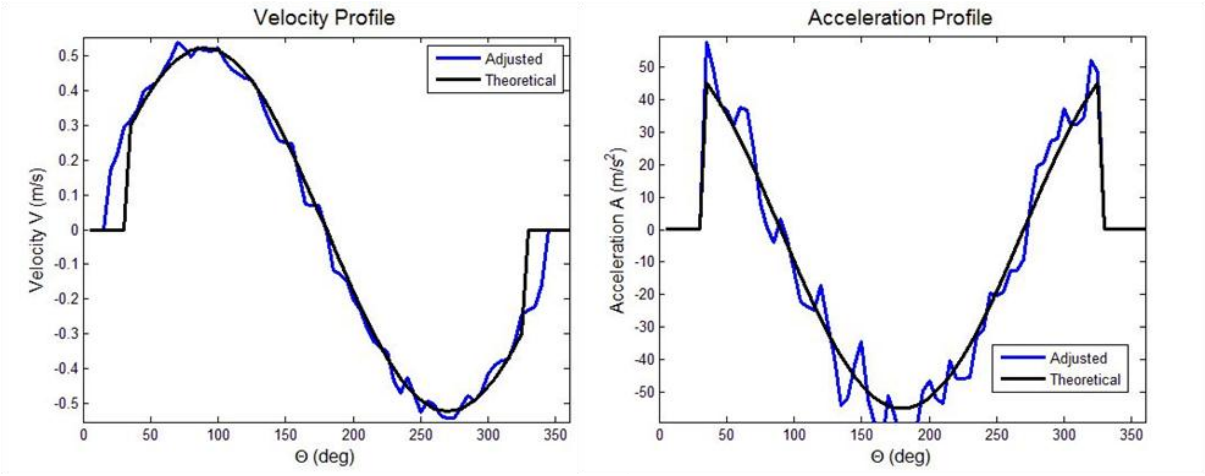

Figure 4.1.2.3: Velocity and acceleration profiles of harmonic cam considering measured curve with a step size of 5˚

4.1.3 3-4-5 Polynomial cam:

3-4-5 Polynomial cam with a RDFD profile was selected. Span of each segment 'β' is π/2.

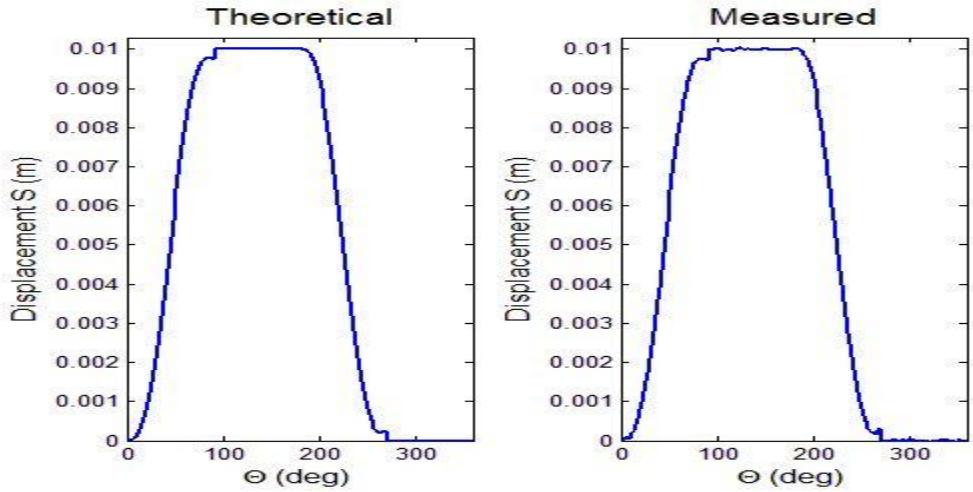

Figure 4.1.3.1: Theoretical and measured displacement profile of 3-4-5 polynomial cam

Figure 4.1.3.1 shows the profile of 3-4-5 polynomial cam before and after adding random errors. Table 4.1.3.1 reveals that deviation of adjusted acceleration from theoretical acceleration corresponding to the angle at maximum theoretical acceleration is lowest at a step size of 6˚. Therefore, this study suggests that selecting step size of 6˚ for a 3-4-5 polynomial cam with a RDFD profile at the specified angular velocity and lift of cam will give relatively more efficient results. Maximum acceleration can be estimated with a percentage error of 1.68% from measured displacement data using adjustment calculus.

Table 4.1.3.1: Deviations at maximum velocity and acceleration of 3-4-5 polynomial cam at different step sizes

Step (degrees)	Percentage Error at maximum theoretical values - mean of n iterations			
	Velocity (m/s)		Acceleration (m/s^2)	
	Unadj	Adj	Unadj	Adj
0.05	1.43E+02	1.40E+02	2.77E+05	2.35E+04
0.1	6.66E+01	6.70E+01	6.69E+04	5.68E+03
0.25	2.74E+01	2.62E+01	1.15E+04	9.36E+02
0.5	1.37E+01	1.36E+01	2.65E+03	2.33E+02
0.75	9.16E+00	9.07E+00	1.28E+03	1.08E+02
1	7.04E+00	6.86E+00	6.98E+02	5.91E+01
2	3.57E+00	3.41E+00	1.70E+02	1.83E+01
3	2.53E+00	2.42E+00	8.07E+01	1.10E+01
5	1.75E+00	2.04E+00	2.88E+01	4.21E+00
6	1.74E+00	1.18E+00	2.07E+01	1.68E+00
9	3.10E+00	4.57E+00	8.36E+00	3.38E+00
10	3.49E+00	7.60E-01	7.08E+00	3.89E+01
15	6.13E+01	1.20E+02	3.66E+02	5.57E+01

Figure 4.1.3.2 displays the systematic errors in velocity and acceleration profile and Figure 4.1.3.3 displays the total errors.

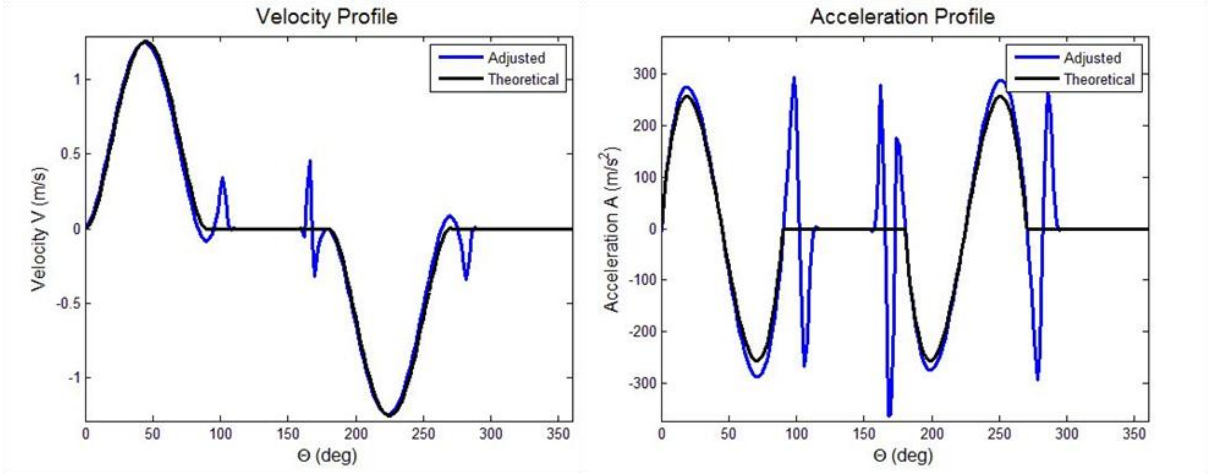

Figure 4.1.3.2: Velocity and acceleration profiles of 3-4-5 polynomial cam considering theoretical curve with a step size of 2˚

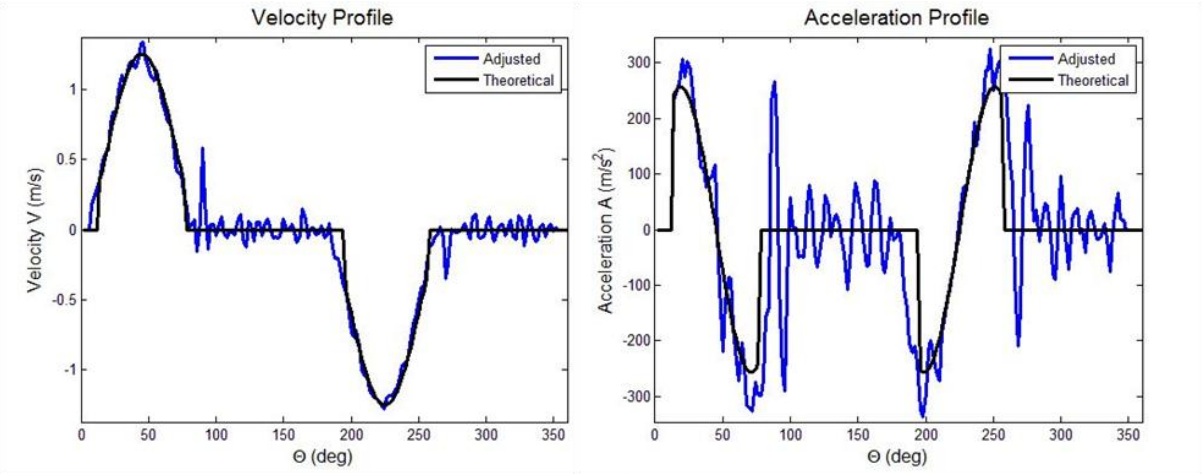

Figure 4.1.3.3: Velocity and acceleration profiles of 3-4-5 polynomial cam considering measured curve with a step size of 2˚

4.1.4 Polynomial cam P1P2:

An 8^{th} order polynomial cam with a DRFD profile was selected. Span of each segment 'β' was π/2.

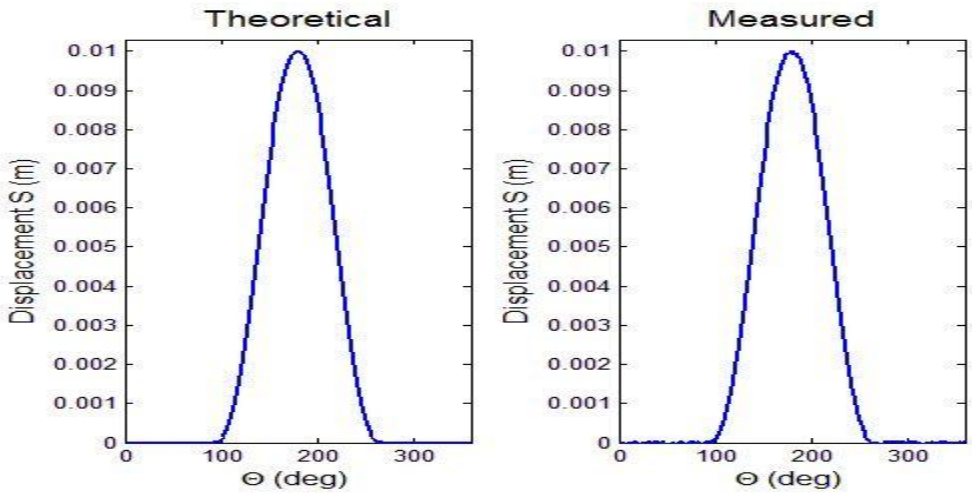

Figure 4.1.4.1: Theoretical and measured displacement profile of polynomial cam P1P2

Figure 4.1.4.1 shows the profile of polynomial cam P1P2 before and after adding random errors. Table 4.1.4.1 reveals that deviation of adjusted acceleration from theoretical acceleration corresponding to the angle at maximum theoretical acceleration is lowest at a step size of 10˚. Therefore, this study suggests that selecting step size of 10˚ for a polynomial cam P1P2 with a DRFD profile at the specified angular velocity and lift of cam will give relatively more efficient results. Maximum acceleration can be estimated with a percentage error of 3.71% from measured displacement data using adjustment calculus.

Table 4.1.4.1: Deviations at maximum velocity and acceleration of polynomial cam P1P2 at different step sizes

Step (degrees)	Percentage Error at maximum theoretical values - mean of n iterations			
	Velocity (m/s)		Acceleration (m/s^2)	
	Unadj	Adj	Unadj	Adj
0.05	1.03E+02	1.01E+02	3.12E+05	2.54E+04
0.1	1.01E+02	9.98E+01	7.36E+04	6.18E+03
0.25	9.96E+01	9.97E+01	1.21E+04	1.02E+03
0.5	1.00E+02	1.00E+02	3.13E+03	2.54E+02
0.75	9.99E+01	1.00E+02	1.30E+03	1.13E+02
1	9.98E+01	9.97E+01	7.72E+02	6.44E+01
2	1.00E+02	1.00E+02	1.92E+02	1.79E+01
3	1.00E+02	1.00E+02	8.87E+01	1.06E+01
5	1.00E+02	1.00E+02	3.11E+01	8.51E+00
6	1.00E+02	1.00E+02	2.14E+01	7.85E+00
9	1.01E+02	1.00E+02	1.00E+01	5.17E+00
10	1.01E+02	1.00E+02	7.51E+00	3.71E+00
15	6.54E+00	1.37E+01	3.55E+00	8.92E+00
18	8.54E+00	5.38E+00	2.44E+00	2.03E+01

Figure 4.1.4.2 displays the systematic errors in velocity and acceleration profile and Figure 4.1.4.3 displays the total errors.

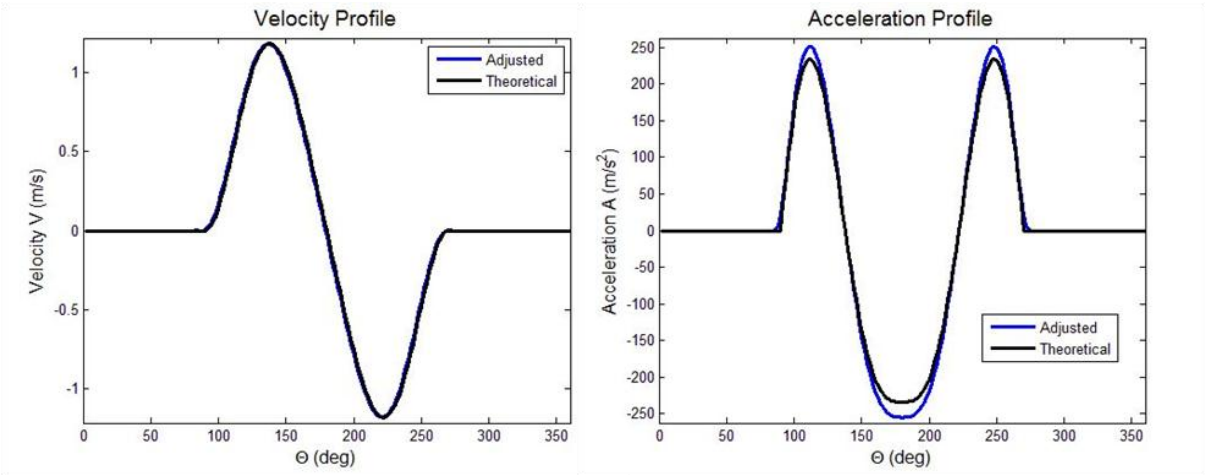

Figure 4.1.4.2: Velocity and acceleration profiles of polynomial cam P1P2 considering theoretical curve with a step size of 5˚

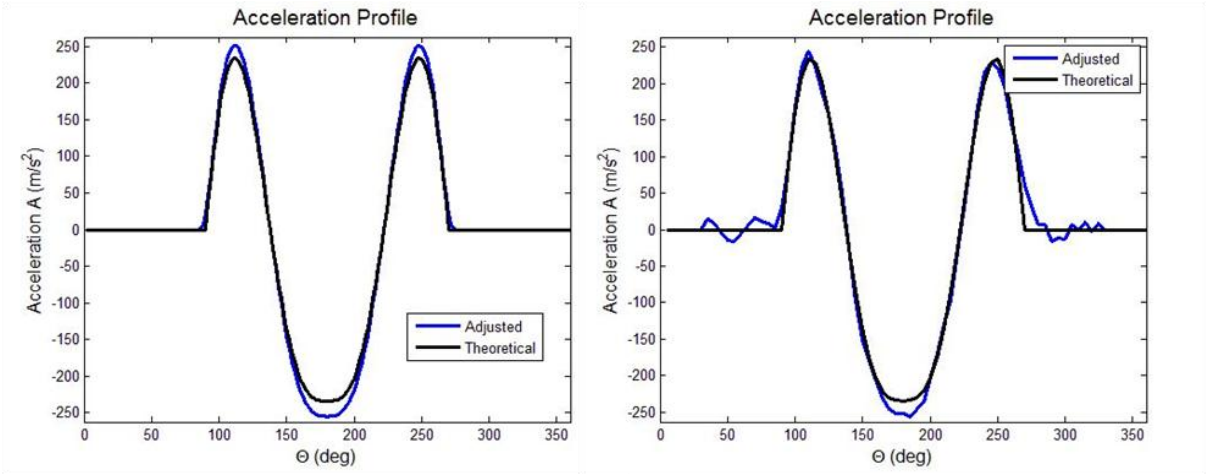

Figure 4.1.4.3: Velocity and acceleration profiles of polynomial cam P1P2 considering measured curve with a step size of 5˚

4.1.5 4-5-6-7 Polynomial cam:

4-5-6-7 Polynomial cam with DRFD profile was selected. Span of each segment 'β' was π/2.

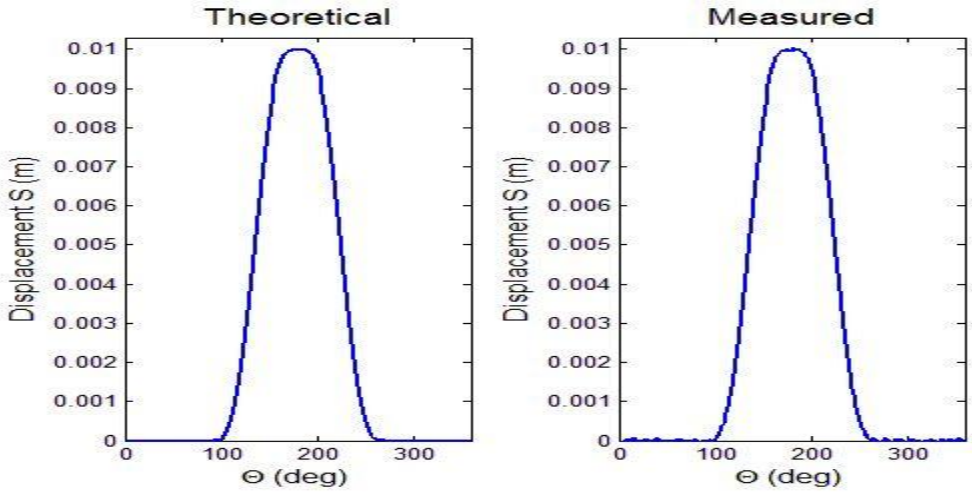

Figure 4.1.5.1: Theoretical and measured displacement profile of 4-5-6-7 polynomial cam

Figure 4.1.5.1 shows the profile of 4-5-6-7 polynomial cam before and after adding random errors. Table 4.1.5.1 reveals that deviation of adjusted acceleration from theoretical acceleration corresponding to the angle at maximum theoretical acceleration is lowest at a step size of 5˚. Therefore, this study suggests that selecting step size of 5˚ for a 4-5-6-7 polynomial cam with a DRFD profile at the specified angular velocity and lift of cam will give relatively more efficient results. Maximum acceleration can be estimated with a percentage error of 4.23% from measured displacement data using adjustment calculus.

Table 4.1.5.1: Deviations at maximum velocity and acceleration of 4-5-6-7 polynomial cam at different step sizes

Step (degrees)	Percentage Error at maximum theoretical values - mean of n iterations			
	Velocity (m/s)		Acceleration (m/s^2)	
	Unadj	Adj	Unadj	Adj
0.05	1.17E+02	1.13E+02	2.04E+05	1.75E+04
0.1	5.77E+01	5.79E+01	5.26E+04	4.41E+03
0.25	2.40E+01	2.25E+01	8.23E+03	7.06E+02
0.5	1.18E+01	1.17E+01	2.07E+03	1.75E+02
0.75	7.94E+00	7.71E+00	9.90E+02	7.87E+01
1	5.95E+00	5.87E+00	5.22E+02	4.37E+01
2	2.98E+00	2.76E+00	1.31E+02	1.21E+01
3	2.00E+00	1.94E+00	5.80E+01	5.94E+00
5	1.51E+00	1.89E+00	2.12E+01	4.23E+00
6	1.75E+00	9.50E-01	1.50E+01	9.59E+00
9	3.91E+00	5.84E+00	7.48E+00	2.94E+01
10	4.59E+00	6.03E-01	7.04E+00	2.96E+01
15	1.04E+01	1.56E+01	1.09E+01	6.40E+01

Figure 4.1.5.2 displays the systematic errors in velocity and acceleration profile and Figure 4.1.5.3 displays the total errors.

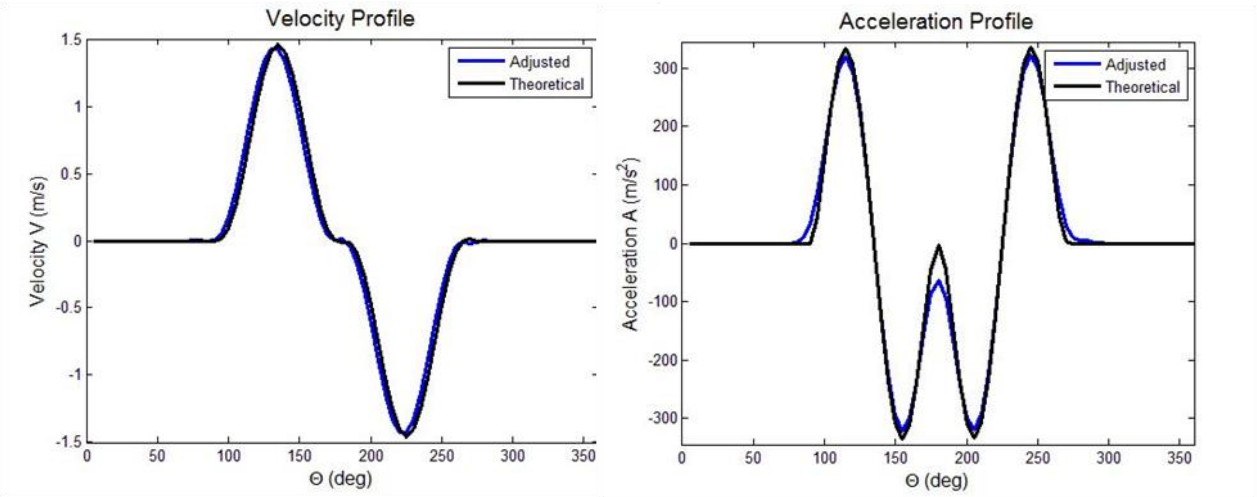

Figure 4.1.5.2: Velocity and acceleration profiles of 4-5-6-7 polynomial cam considering theoretical curve with a step size of 5˚

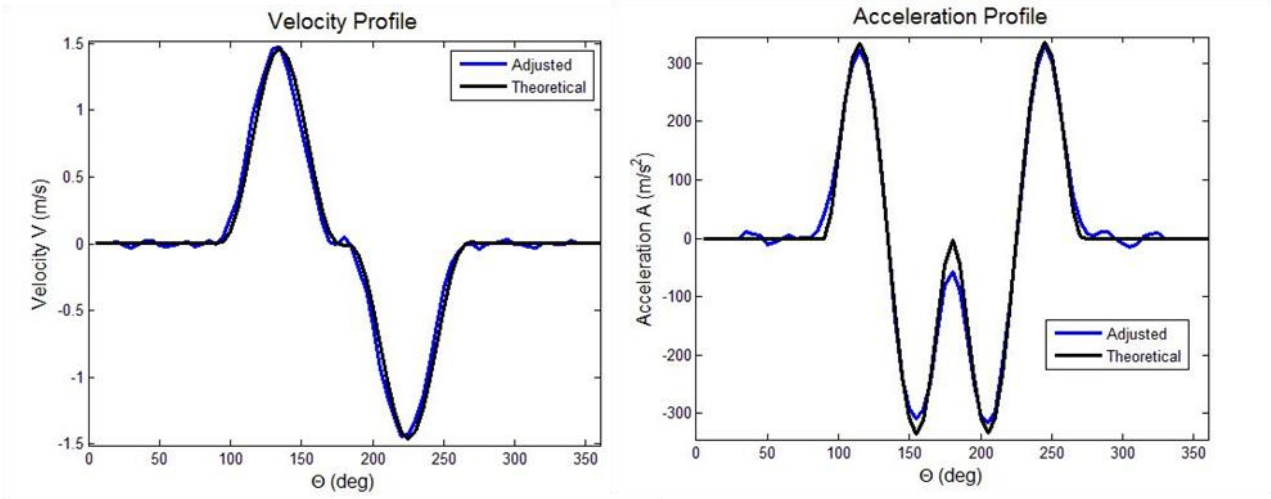

Figure 4.1.5.3: Velocity and acceleration profiles of 4-5-6-7 polynomial cam considering measured curve with a step size of 5˚

4.1.6 Modified Trapezoidal cam:

A Modified Trapezoidal cam with a DRFD profile was selected. Span of each dwell 'β_1' was $\pi/3$. Span of rise and fall 'β_2' was each $2\pi/3$.

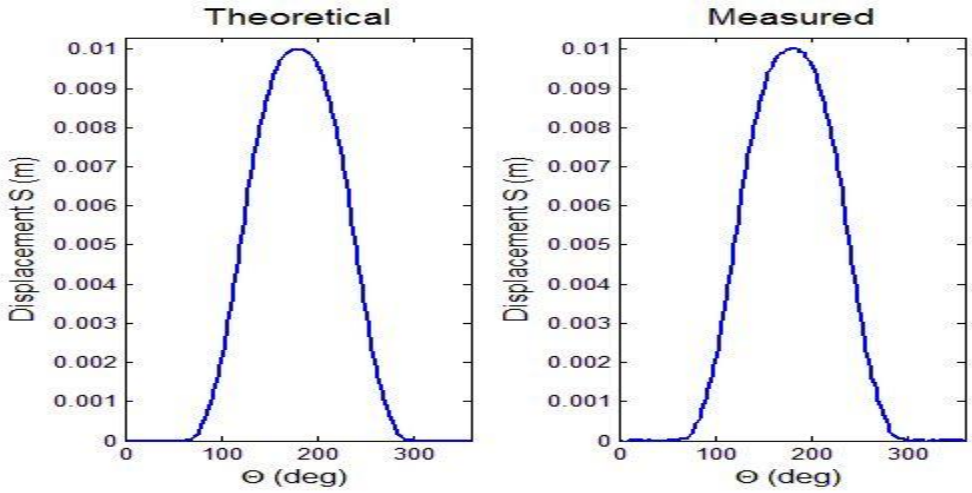

Figure 4.1.6.1: Theoretical and measured displacement profile of modified trapezoidal cam

Figure 4.1.6.1 shows the profile of modified trapezoidal cam before and after adding random errors. Table 4.1.6.1 reveals that deviation of adjusted acceleration from theoretical acceleration corresponding to the angle at maximum theoretical acceleration is lowest at a step size of 5˚. Therefore, this study suggests that selecting step size of 5˚ for a modified trapezoidal cam with a DRFD profile at the specified angular velocity and lift of cam will give relatively more efficient results. Maximum acceleration can be estimated with a percentage error of 5.17% from measured displacement data using adjustment calculus.

Table 4.1.6.1: Deviations at maximum velocity and acceleration of modified trapezoidal cam at different step sizes

Step (degrees)	Percentage Error at maximum theoretical values - mean of n iterations			
	Velocity (m/s)		Acceleration (m/s^2)	
	Unadj	Adj	Unadj	Adj
0.05	1.68E+02	1.70E+02	5.90E+05	4.76E+04
0.1	8.33E+01	8.49E+01	1.47E+05	1.27E+04
0.25	3.35E+01	3.35E+01	2.31E+04	1.93E+03
0.5	1.71E+01	1.62E+01	6.05E+03	4.76E+02
0.75	1.16E+01	1.14E+01	2.59E+03	2.20E+02
1	8.53E+00	8.33E+00	1.48E+03	1.19E+02
3	2.89E+00	2.95E+00	1.66E+02	1.42E+01
5	1.82E+00	1.94E+00	5.97E+01	5.17E+00
7.5	2.07E+00	2.94E+00	2.66E+01	1.23E+01

Figure 4.1.6.2 displays the systematic errors in velocity and acceleration profile and Figure 4.1.6.3 displays the total errors.

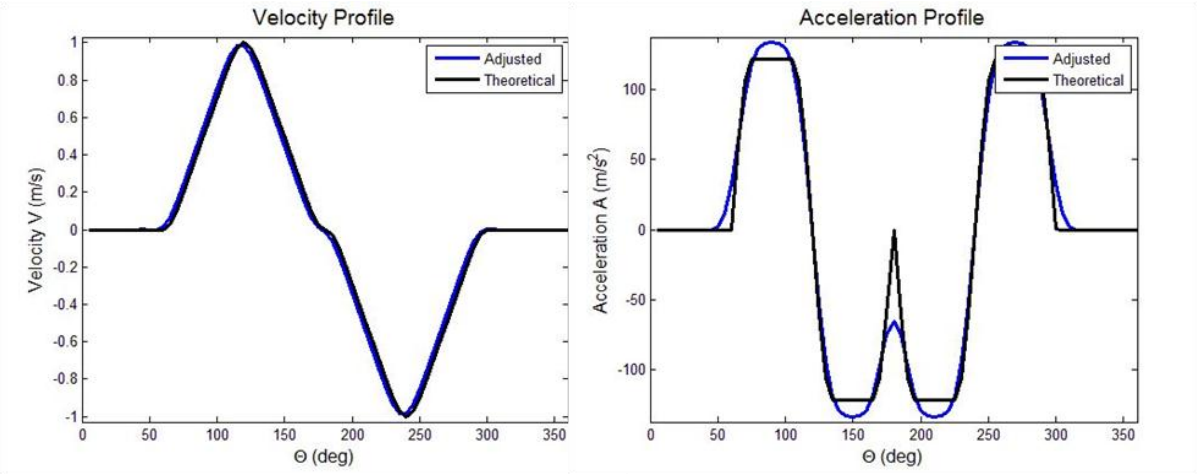

Figure 4.1.6.2: Velocity and acceleration profiles of modified trapezoidal cam considering theoretical curve with a step size of 5˚

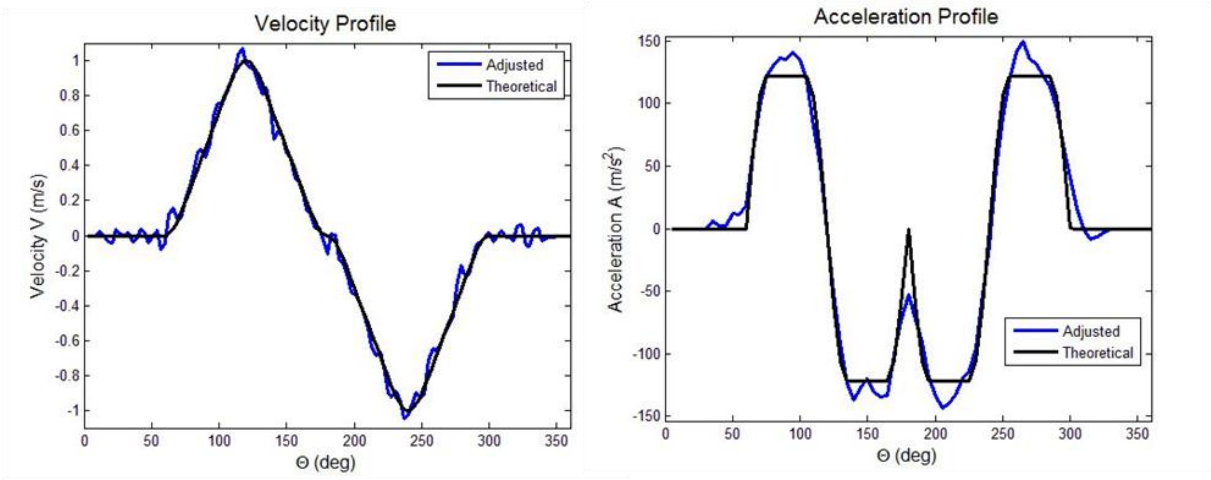

Figure 4.1.6.3: Velocity and acceleration profiles of modified trapezoidal cam considering measured curve with a step size of 5˚

4.1.7 Sine cam:

A Sine cam with RFR profile was considered. Span of each segment 'β' was π.

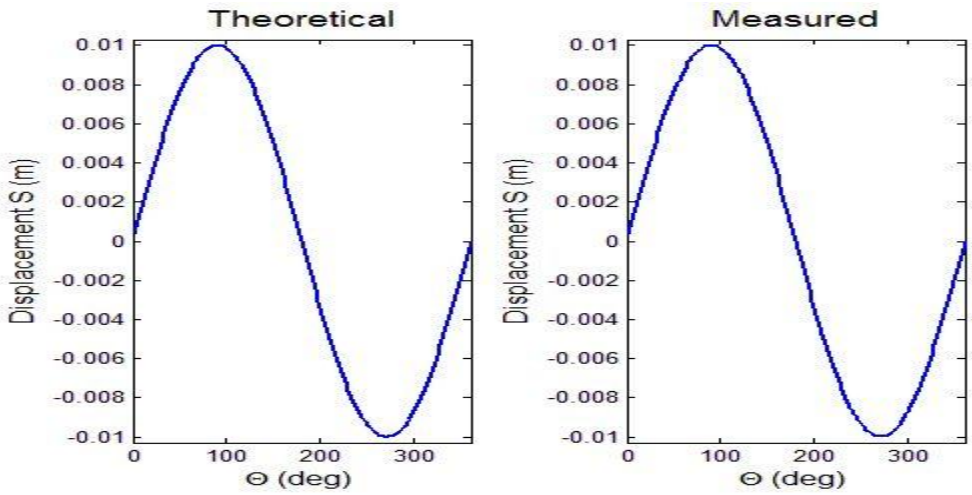

Figure 4.1.7.1: Theoretical and measured displacement profile of sine cam

Figure 4.1.7.1 shows the profile of sine cam before and after adding random errors. Table 4.1.7.1 reveals that deviation of adjusted acceleration from theoretical acceleration corresponding to the angle at maximum theoretical acceleration decreases with increase in step size. This study does not suggest a specific step size for a sine cam with a RFR profile at the specified angular velocity and lift of cam. A step size of 12˚ gives the best results in this study. Maximum acceleration can be estimated with a percentage error of 5.15% from measured displacement data using adjustment calculus.

Table 4.1.7.1: Deviations at maximum velocity and acceleration of sine cam at different step sizes

Step (degrees)	Percentage Error at maximum theoretical values - mean of n iterations			
	Velocity (m/s)		Acceleration (m/s^2)	
	Unadj	Adj	Unadj	Adj
0.05	1.60E+02	1.57E+02	6.47E+05	5.33E+04
0.1	8.11E+01	8.12E+01	1.62E+05	1.37E+04
0.25	3.30E+01	3.21E+01	2.68E+04	2.25E+03
0.5	1.54E+01	1.51E+01	6.20E+03	5.33E+02
0.75	1.09E+01	1.04E+01	2.92E+03	2.50E+02
1	8.55E+00	8.05E+00	1.68E+03	1.29E+02
2	4.04E+00	3.95E+00	3.96E+02	3.49E+01
3	2.62E+00	2.59E+00	1.83E+02	1.64E+01
5	1.64E+00	1.56E+00	6.58E+01	8.97E+00
6	1.33E+00	1.33E+00	4.45E+01	8.26E+00
9	9.70E-01	1.03E+00	2.08E+01	6.71E+00
10	9.31E-01	1.03E+00	1.62E+01	6.26E+00
12	9.40E-01	1.18E+00	1.19E+01	5.15E+00

Figure 4.1.7.2 displays the systematic errors in velocity and acceleration profile and Figure 4.1.7.3 displays the total errors.

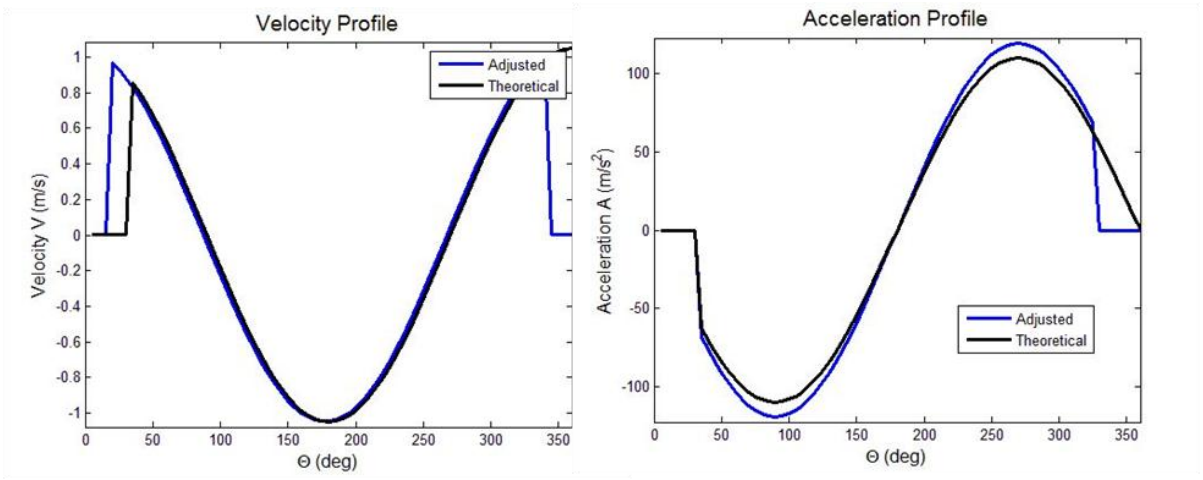

Figure 4.1.7.2: Velocity and acceleration profiles of sine cam considering theoretical curve with a step size of 5˚

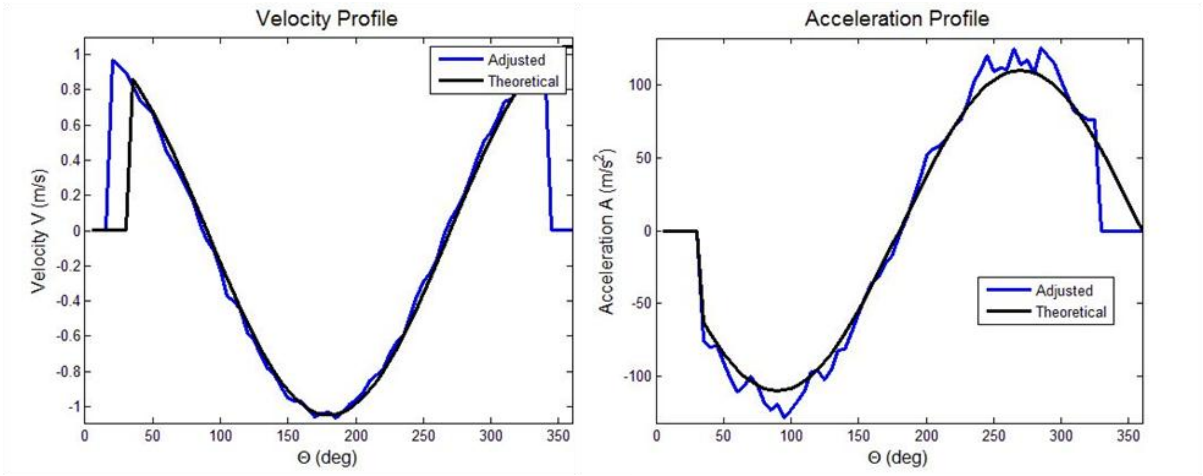

Figure 4.1.7.3: Velocity and acceleration profiles of sine cam considering measured curve with a step size of 5˚

4.2 Effect of dwell location on step size

The effect of location of dwell on effective step size selection will be studied. Monte Carlo Simulations will be implemented for a Cycloidal cam, 3-4-5 Polynomial cam and 4-5-6-7 Polynomial cam. Monte Carlo Simulations will be carried similar to section 4.1. Values of the variables 'L', 'ω', 'n' and randomness of errors will be fixed as considered in section 4.1. Results of this study will be compared to the results in section 4.1 for analysis.

4.2.1 Cycloidal Cam:

A RDFD profile was considered in section 4.1.1. In this study, DRFD profile will considered for the cycloidal cam. The span 'β' will be fixed at π/2 for each segment.

Table 4.2.1.1: Deviations at maximum velocity and acceleration of cycloidal cam at different step sizes

Step (degrees)	Percentage Error at maximum theoretical values - mean of n iterations			
	Velocity (m/s)		Acceleration (m/s^2)	
	Unadj	Adj	Unadj	Adj
0.75	8.69E+00	8.46E+00	1.19E+03	9.28E+01
1	6.48E+00	6.33E+00	6.30E+02	5.24E+01
2	3.24E+00	3.06E+00	1.60E+02	1.54E+01
3	2.22E+00	2.14E+00	7.13E+01	7.45E+00
5	1.54E+00	1.76E+00	2.62E+01	2.57E+00
6	1.57E+00	1.03E+00	1.78E+01	6.31E+00

From Table 4.2.1.1, we can infer that step size of 5˚ is the optimum step in this case. It can also be inferred that location of dwell does not influence effective step size selection (Tables 4.1.1.1 and 4.2.1.1). Optimum step size for RDFD profile was found to be 5˚.

4.2.2 3-4-5 Polynomial Cam:

A RDFD profile was considered in section 4.1.3. In this study, DRFD profile will be considered for the 3-4-5 polynomial cam. The span 'β' will be fixed at π/2 for each segment.

Table 4.2.2.1: Deviations at maximum velocity and acceleration of 3-4-5 polynomial cam at different step sizes

Step (degrees)	Percentage Error at maximum theoretical values - mean of n iterations			
	Velocity (m/s)		Acceleration (m/s^2)	
	Unadj	Adj	Unadj	Adj
0.75	9.38E+00	9.11E+00	1.17E+03	1.07E+02
1	7.10E+00	6.71E+00	7.00E+02	6.03E+01
2	3.52E+00	3.45E+00	1.78E+02	1.77E+01
3	2.41E+00	2.32E+00	7.92E+01	1.08E+01
5	1.69E+00	1.97E+00	2.81E+01	4.21E+00
6	1.74E+00	1.24E+00	1.92E+01	3.70E+00
9	3.12E+00	4.63E+00	8.85E+00	2.32E+01

Table 4.2.2.1 infers that the optimum step size is 6˚. Table 4.1.3.1 infers that location of dwell does not influence the optimum step size for this cam profile.

4.2.3 4-5-6-7 Polynomial Cam:

A DRFD profile was considered in section 4.1.5. In this study, a RDFD profile will considered for cycloidal cam. The span 'β' will be fixed at π/2 for each segment.

Table 4.2.3.1: Deviations at maximum velocity and acceleration of 4-5-6-7 polynomial cam at different step sizes

Step (degrees)	Percentage Error at maximum theoretical values - mean of n iterations			
	Velocity (m/s)		Acceleration (m/s^2)	
	Unadj	Adj	Unadj	Adj
0.75	7.54E+00	7.66E+00	9.65E+02	7.87E+01
1	5.84E+00	5.54E+00	5.21E+02	4.44E+01
2	2.96E+00	2.99E+00	1.32E+02	1.28E+01
3	2.00E+00	1.94E+00	6.02E+01	6.06E+00
5	1.56E+00	1.95E+00	2.13E+01	4.32E+00
6	1.92E+00	1.00E+00	1.39E+01	9.56E+00

Table 4.2.3.1 infers that the optimum step size is 5˚. Tables 4.1.5.1 and 4.2.3.1 suggest that there is no influence of dwell location on optimum step size selection for this profile.

5. CONCLUSIONS AND FUTURE WORK

5.1 Conclusions:

Application of a little known method developed by J. Oderfeld [19] has been discussed at length in this work. This procedure has been compared with other existing methods. A procedure to implement adjustment calculus and Monte Carlo methods to any cam profile has been discussed. Weights for calculation of adjusted velocity have been derived in chapter 2 using a cubic polynomial fit and the Symmetric Stirling interpolation formula. Its application for Monte Carlo simulations has been discussed in chapters 3 & 4.

5.1.1 Effect of profile type on optimum step selection:

In section 4.1, effect of step size on velocity and acceleration profiles has been discussed. This investigation shows that profile type has an influence on optimum step

size selection. Optimum step size for various profiles has been suggested. The value of standard deviation of errors considered is 0.0000254 m with a mean of 0. An angular velocity of 104.71 rad/s that corresponds to 1000 rpm which classifies the cam to be a high speed cam.

The maximum acceleration of a cycloidal cam (RDFD profile) with a lift of 0.01 m and rotating at an angular velocity of 104.71 rad/s can be estimated with an error of 2.42% using adjustment calculus when a step size of 5˚. Similarly, for a harmonic cam (RFR profile) with a lift of 0.01 m and rotating at an angular velocity of 104.71 rad/s, maximum acceleration can be estimated with an error of 0.88% when a step size of 18˚ is considered. A step size smaller than 18˚, can be considered by the user if slightly larger error is acceptable.

Three polynomial cams were considered with a lift of 0.01 m and rotating at an angular velocity of 104.71 rad/s. For a 3-4-5 polynomial cam (RDFD profile), adjustment calculus can be used to find the maximum acceleration from displacement data with an error of 1.68% by considering a step size of 6˚. A step size of 10˚ was found to be optimum for an 8^{th} order polynomial cam P1P2 (DRFD profile). Maximum acceleration can be found with a 3.71% error for this cam. For a 4-5-6-7 polynomial cam (DRFD profile), a step size of 5˚ was found to be optimum and the maximum acceleration can be predicted with an error of 4.23% using this step size.

A modified trapezoidal cam (DRFD) cam was considered with a lift of 0.01 m and angular velocity of 104.71 rad/s. 5˚ was found to be optimum step size selection.

Maximum acceleration can be estimated with an error of 5.17% using adjustment calculus.

An optimum step size was not conclusive for a sine cam (RFR profile) with a lift of 0.01 m and an angular velocity of 104.71 rad/s. An increase in step resulted in decrease in error. Maximum acceleration can be estimated with an error of 5.15% when a step size of 12˚ is considered.

5.1.2 Effect of location of dwell on optimum step selection:

In section 4.2, effect of location of dwell within the profile on optimum step size selection has been discussed for three cam profiles cycloidal cam, 3-4-5 polynomial cam and 4-5-6-7 polynomial cam. This study inferred that the location of dwell has no impact on optimum step size selection for all the three cam profiles that were analyzed.

This investigation has emphasized the importance of studying the optimum step size to apply adjustment calculus for velocity and acceleration estimations in quality control of cams. This method can also be used for other applications discussed in this work. Velocity and acceleration can be estimated by considering displacement data. This method can be applied immediately after collecting few displacement positions. Therefore, this procedure can be used for real time analysis and predictions.

5.2 Future Work

This work can be extended to study the impact of other variables like span of each segment of the profile 'β', angular velocity 'ω' and lift of cam 'L' on optimum step selection can be studied.

Change in angular velocity 'ω' will change the step size. Therefore, the effect of changing angular velocity can be extrapolated from this study. An increase in angular velocity would result in reduction of time step size and thus the optimum step size would be a smaller value than the ones suggested in this study. Similarly, a smaller angular velocity would result in an optimum step size greater in value than the step size suggested in this study. This phenomenon can be validated in future study.

Lift of the cam 'L' proportionally alters the values of velocity and acceleration. According to this study, there should not be any influence of lift of the cam 'L' on optimum step size selection. This phenomenon can also be validated in future.

'Weights' for calculation of adjusted acceleration in this study was derived with a cubic polynomial. Ming-Feng Jean [4] derived weights for acceleration considering higher order polynomials. The effect of these weights can be studied on acceleration predictions.

A cubic polynomial was used to derive weights for adjusted velocity calculation. Higher order polynomial can be used to derive weights and effect of adjustment on velocity predictions can be studied.

As discussed earlier, this technique can be implemented for quality control of cams. This technique can also be used where velocity and acceleration needs to be calculated

from displacement data as mentioned in section 1.3. Therefore application of this technique can be embedded into software which can provide a user friendly interface.

References

1. John R. Taylor, “An introduction to error analysis: The study of uncertainties in physical measurements”, 2nd edition (1997)
2. Harold A. Rothbart, “Cam Manufacturing”, Cam Design Handbook, McGraw-Hill (2004**)**
3. John J. Uicker Jr., Gordon R. Pennock, Joseph E. Shigley, “Theory of Machines and Mechanisms”, Oxford University Press, (2011)
4. Ming-Feng Jean, “Determination of the velocity and acceleration by the Adjustment Calculus” Thesis presented at University of Nebraska-Lincoln, (1994)
5. Andrea Bonarini, Paolo Aliverti, Michele Lucioni, “An omnidirectional vision sensor for fast tracking for mobile robots”, IEEE Transactions on Instrumentation and Measurement, **49** (2000) 509-512
6. M Futatskua, N Yasutake, T Sakurai and T Matsumoto, "Comparative study of vibration disease among operators of vibrating tools by factor analysis", British Journal of Industrial Medicine, (1985)
7. Barbara Harazin, Agnieszka Harazin-Lechowska, Jacek Kalamarz, Grzegorz Zielinski, “Measurements of vibrotactile perception thresholds at the fingertips in Poland”, Industrial Health, **43** (2005) 535-541
8. Emily Geist, Kenji Shimada, “Position error reduction in a mechanical tracking linkage for arthroscopic hip surgery”, Int J CARS, **6** (2011) 693-698
9. Vassilios Gourgoulis, Nikolaos Aggeloussis, Panagiotis Kasimatis, Nikolaos Vezos, Alexia Boli, Giorgos Mavromatis, “Reconstruction accuracy in

underwater three-dimensional kinematic analysis", Journal of Science and Medicine in Sport,**11** (2008) 90-95

10. U. Rauhala, "Nonlinear array algebra in digital photogrammetry", ISPRS, **29** (1992) 95-102
11. EC Firth, CW Rogers, NR Perkins, BH Anderson, ND Grace, "Musculoskeletal responses of 2-year-old Thoroughbred horses to early training. 1. Study design, and clinical, nutritional, radiological and histological observations", N Z Vet J., **52** (2004) 261-271
12. Johnson, R.C., "Method of finite differences provides simple but flexible arithmatical techniques for cam design", Mach. Des. Nov., (1955) 195-204.
13. J.H. Nourse, "Recent Developments in Cam Profile Measurement and Evaluation", Society of Automotive Engineers, IAEC, Jan 11-15 (1965) 1-46
14. J.H.C Brittain, R. Horsnell, "A Prediction of Some Causes and Effects of Cam Profile Errors", Proceedings of the Institution of Mechanical Engineers, **183** 3L (1967-68) 145-151
15. P.S. Grewal, W.R. Newcombe, "Dynamic Performance of High Speed Semi-Rigid Follower Cam Systems – Effects of Cam Profile Errors", Mechanism and Machine Theory, Pergamon Press Limited, **23** (1988) 121-133
16. F.Y. Chen, "Mechanics and Design of Cam Mechanisms", Pergamon Press, New York, (1982)
17. James M.L., Smith G.M., Wolford J.C., "Applied Numerical Methods for Digital Computation", Harper Collins College Publishers, New York, (1993)

18. F.Y. Chen, “An algorithm for computing the contour of a slow speed cam”, J. Mech., **4** (1969) 171-175
19. J. Oderfeld, “Wstep Do Mechanicznej Teorii Maszyn Wnt”, (In Polish, ‘Introduction to Mechanical Theory of Machines’), (1962)
20. I. N. Bronshtein, K. A. Semendyayev, “Handbook of Mathematics”, Van Nostrand Reinhold, New York, (1985)
21. Richard L. Burden, J. Douglas Faires, “Numerical Analysis”, PWS-KENT Publishing Company, Boston, (1993)
22. Jan J. Tuma, “Handbook of Numerical Calculations in Engineering”, McGraw-Hill Book Company, New York, (1989)
23. Nicholas Metropolis, Ulam S., “The Monte Carlo method”, Journal of the American Statistical Association, **44** (1949) 335-341

Appendix 1

```
> restart;
>
> d[-3] := (f[i-3] - (c3*(-3*h)^3 + c2*(-3*h)^2 + c1*(-3*h) + c0))^2;

                    d[-3] := (f[i - 3] + 27 c3 h^3 - 9 c2 h^2 + 3 c1 h - c0)^2

> d[-2] := (f[i-2] - (c3*(-2*h)^3 + c2*(-2*h)^2 + c1*(-2*h) + c0))^2;

                     d[-2] := (f[i - 2] + 8 c3 h^3 - 4 c2 h^2 + 2 c1 h - c0)^2

> d[-1] := (f[i-1] - (c3*(-h)^3 + c2*(-h)^2 + c1*(-h) + c0))^2;

                        d[-1] := (f[i - 1] + c3 h^3 - c2 h^2 + c1 h - c0)^2

> d[0] := (f[i] - c0)^2;

                                  d[0] := (f[i] - c0)^2

> d[1] := (f[i+1] - (c3*(h)^3 + c2*(h)^2 + c1*(h) + c0))^2;

                        d[1] := (f[i + 1] - c3 h^3 - c2 h^2 - c1 h - c0)^2

> d[2] := (f[i+2] - (c3*(2*h)^3 + c2*(2*h)^2 + c1*(2*h) + c0))^2;

                     d[2] := (f[i + 2] - 8 c3 h^3 - 4 c2 h^2 - 2 c1 h - c0)^2

> d[3] := (f[i+3] - (c3*(3*h)^3 + c2*(3*h)^2 + c1*(3*h) + c0))^2;

                     d[3] := (f[i + 3] - 27 c3 h^3 - 9 c2 h^2 - 3 c1 h - c0)^2

> error := d[-3] + d[-2] + d[-1] + d[0] + d[1] + d[2] + d[3];

error := (f[i - 3] + 27 c3 h^3 - 9 c2 h^2 + 3 c1 h - c0)^2

      + (f[i - 2] + 8 c3 h^3 - 4 c2 h^2 + 2 c1 h - c0)^2

      + (f[i - 1] + c3 h^3 - c2 h^2 + c1 h - c0)^2 + (f[i] - c0)^2

      + (f[i + 1] - c3 h^3 - c2 h^2 - c1 h - c0)^2

      + (f[i + 2] - 8 c3 h^3 - 4 c2 h^2 - 2 c1 h - c0)^2

      + (f[i + 3] - 27 c3 h^3 - 9 c2 h^2 - 3 c1 h - c0)^2

> e1 := diff(error,c3);

e1 := 54 (f[i - 3] + 27 c3 h^3 - 9 c2 h^2 + 3 c1 h - c0) h^3
```

```
      + 16 (f[i - 2] + 8 c3 h^3 - 4 c2 h^2 + 2 c1 h - c0) h^3

      + 2 (f[i - 1] + c3 h^3 - c2 h^2 + c1 h - c0) h^3

      - 2 (f[i + 1] - c3 h^3 - c2 h^2 - c1 h - c0) h^3

      - 16 (f[i + 2] - 8 c3 h^3 - 4 c2 h^2 - 2 c1 h - c0) h^3

      - 54 (f[i + 3] - 27 c3 h^3 - 9 c2 h^2 - 3 c1 h - c0) h^3
> e2 := diff(error,c2);

e2 := -18 (f[i - 3] + 27 c3 h^3 - 9 c2 h^2 + 3 c1 h - c0) h^2

      - 8 (f[i - 2] + 8 c3 h^3 - 4 c2 h^2 + 2 c1 h - c0) h^2

      - 2 (f[i - 1] + c3 h^3 - c2 h^2 + c1 h - c0) h^2

      - 2 (f[i + 1] - c3 h^3 - c2 h^2 - c1 h - c0) h^2

      - 8 (f[i + 2] - 8 c3 h^3 - 4 c2 h^2 - 2 c1 h - c0) h^2

      - 18 (f[i + 3] - 27 c3 h^3 - 9 c2 h^2 - 3 c1 h - c0) h^2
> e3 := diff(error,c1);

e3 := 6 (f[i - 3] + 27 c3 h^3 - 9 c2 h^2 + 3 c1 h - c0) h

      + 4 (f[i - 2] + 8 c3 h^3 - 4 c2 h^2 + 2 c1 h - c0) h

      + 2 (f[i - 1] + c3 h^3 - c2 h^2 + c1 h - c0) h

      - 2 (f[i + 1] - c3 h^3 - c2 h^2 - c1 h - c0) h

      - 4 (f[i + 2] - 8 c3 h^3 - 4 c2 h^2 - 2 c1 h - c0) h

      - 6 (f[i + 3] - 27 c3 h^3 - 9 c2 h^2 - 3 c1 h - c0) h
> e4 := diff(error,c0);

e4 := -2 f[i - 3] - 2 f[i - 2] - 2 f[i - 1] + 56 c2 h^2 + 14 c0

      - 2 f[i + 3] - 2 f[i + 2] - 2 f[i] - 2 f[i + 1]
```

```
> sol := solve({e1,e2,e3,e4},{c3,c2,c1,c0});

sol := {

    c2 =

                5 f[i - 3] - 3 f[i - 1] - 3 f[i + 1] + 5 f[i + 3] - 4 f[i]
    1/84 ------------------------------------------------------------,
                                          2
                                         h

    c3 = - 1/36

    f[i - 3] - f[i - 2] - f[i - 1] + f[i + 1] + f[i + 2] - f[i + 3]
    ---------------------------------------------------------------,
                                      3
                                     h

    c1 = 1/252 (22 f[i - 3] - 67 f[i - 2] - 58 f[i - 1] + 58 f[i + 1]

     + 67 f[i + 2] - 22 f[i + 3])/h, c0 = - 2/21 f[i - 3]

     + 2/7 f[i - 1] + 2/7 f[i + 1] - 2/21 f[i + 3] + 1/3 f[i]

     + 1/7 f[i - 2] + 1/7 f[i + 2]}

> assign(sol);
> c0;

- 2/21 f[i - 3] + 2/7 f[i - 1] + 2/7 f[i + 1] - 2/21 f[i + 3]

     + 1/3 f[i] + 1/7 f[i - 2] + 1/7 f[i + 2]

> for i from -3 to 3 do y[i] := c0; od;

y[-3] := - 2/21 f[-6] + 2/7 f[-4] + 2/7 f[-2] - 2/21 f[0] + 1/3 f[-3]

     + 1/7 f[-5] + 1/7 f[-1]

y[-2] := - 2/21 f[-5] + 2/7 f[-3] + 2/7 f[-1] - 2/21 f[1] + 1/3 f[-2]

     + 1/7 f[-4] + 1/7 f[0]

y[-1] := - 2/21 f[-4] + 2/7 f[-2] + 2/7 f[0] - 2/21 f[2] + 1/3 f[-1]

     + 1/7 f[-3] + 1/7 f[1]

y[0] := - 2/21 f[-3] + 2/7 f[-1] + 2/7 f[1] - 2/21 f[3] + 1/3 f[0]

     + 1/7 f[-2] + 1/7 f[2]

y[1] := - 2/21 f[-2] + 2/7 f[0] + 2/7 f[2] - 2/21 f[4] + 1/3 f[1]

     + 1/7 f[-1] + 1/7 f[3]

y[2] := - 2/21 f[-1] + 2/7 f[1] + 2/7 f[3] - 2/21 f[5] + 1/3 f[2]

     + 1/7 f[0] + 1/7 f[4]
```

```
y[3] := - 2/21 f[0] + 2/7 f[2] + 2/7 f[4] - 2/21 f[6] + 1/3 f[3]
     + 1/7 f[1] + 1/7 f[5]
> u := x/h;
                                u := x/h
> v2 := (u^2-1)/(3*u);
                                  /  2     \
                                  | x      |
                                  |---- - 1| h
                                  |  2     |
                                  \ h      /
                        v2 := 1/3 ----------
                                     x
> v4 := (u^2-2^2)/(5*u);
                                  /  2     \
                                  | x      |
                                  |---- - 4| h
                                  |  2     |
                                  \ h      /
                        v4 := 1/5 ----------
                                     x
> v6 := (u^2-3^2)/(7*u);
                                  /  2     \
                                  | x      |
                                  |---- - 9| h
                                  |  2     |
                                  \ h      /
                        v6 := 1/7 ----------
                                     x
> w1 := 1/2*(dy[-1/2] + dy[1/2]);
                   w1 := 1/2 dy[-1/2] + 1/2 dy[1/2]
> w3 := 1/2*(d3y[-1/2] + d3y[1/2]);
                  w3 := 1/2 d3y[-1/2] + 1/2 d3y[1/2]
> w5 := 1/2*(d5y[-1/2] + d5y[1/2]);
                  w5 := 1/2 d5y[-1/2] + 1/2 d5y[1/2]
> n := 6;
                                n := 6
> d6y0 := sum((-1)^r*binomial(n,r)*y[n/2-r],r=0..n);
d6y0 := - 2/21 f[-6] - 2 f[-4] - 12/7 f[-2] + 8/3 f[-3] + 5/7 f[-5]
     + 3/7 f[1] - 12/7 f[2] + 8/3 f[3] - 2 f[4] + 5/7 f[5]
     - 2/21 f[6] + 3/7 f[-1]
```

```
> n :=4;
```

$$n := 4$$

```
> d4y0 := sum((-1)^r*binomial(n,r)*y[n/2-r],r=0..n);
```

$$d4y0 := \frac{11}{21} f[-4] + 3/7\, f[-2] - 6/7\, f[-3] - 2/21\, f[-5] + 3/7\, f[2] - 6/7\, f[3] + \frac{11}{21} f[4] - 2/21\, f[5]$$

```
> n := 2;
```

$$n := 2$$

```
> d2y0 := sum((-1)^r*binomial(n,r)*y[n/2-r],r=0..n);
```

$$d2y0 := -2/21\, f[-2] - 2/21\, f[0] - 2/21\, f[2] - 2/21\, f[4] - 2/21\, f[1] - 2/21\, f[-1] + 1/3\, f[3] + 1/3\, f[-3] - 2/21\, f[-4]$$

```
> Y := y[0]+u*(w1+u/2*(d2y0+v2*(w3+u/4*(d4y0+v4*(w5+u/6*(d6y0))))));
```

$$Y := -2/21\, f[-3] + 2/7\, f[-1] + 2/7\, f[1] - 2/21\, f[3] + 1/3\, f[0] + 1/7\, f[-2] + 1/7\, f[2] + x \left| \begin{array}{l} 1/2\ dy[-1/2] + 1/2\ dy[1/2] + 1/2\ x \\ \\ \end{array} \right| - 2/21\, f[-2] - 2/21\, f[0] - 2/21\, f[2] - 2/21\, f[4] - 2/21\, f[1] - 2/21\, f[-1] + 1/3\, f[3] + 1/3\, f[-3] - 2/21\, f[-4] + 1/3 \left(\frac{x^2}{h^2} - 1 \right) h \left| \begin{array}{l} 1/2\ d3y[-1/2] + 1/2\ d3y[1/2] + 1/4\ x \\ \\ \end{array} \right| \frac{11}{21} f[-4] + 3/7\, f[-2] - 6/7\, f[-3] - 2/21\, f[-5] + 3/7\, f[2] - 6/7\, f[3] + \frac{11}{21} f[4] - 2/21\, f[5] + 1/5 \left(\frac{x^2}{h^2} - 4 \right) h\ (1/2\ d5y[-1/2] + 1/2\ d5y[1/2] + 1/6\, x\, (-2/21\, f[-6] - 2\, f[-4] - 12/7\, f[-2] + 8/3\, f[-3] + 5/7\, f[-5] + 3/7\, f[1] - 12/7\, f[2] + 8/3\, f[3] - 2\, f[4] + 5/7\, f[5] - 2/21\, f[6] + 3/7\, f[-1])/h)/x \left| \begin{array}{l} /h \\ \\ \end{array} \right| /x \left| \begin{array}{l} /h \\ \\ \end{array} \right| /h$$

```
> Y1 := diff(Y,x);
```

$$
\begin{aligned}
Y1 := {} & \int \tfrac{1}{2}\,dy_{-1/2} + \tfrac{1}{2}\,dy_{1/2} + \tfrac{1}{2}\,x \,\Big|_{-} \tfrac{2}{21} f_{-2} - \tfrac{2}{21} f_{0} \\
& - \tfrac{2}{21} f_{2} - \tfrac{2}{21} f_{4} - \tfrac{2}{21} f_{1} - \tfrac{2}{21} f_{-1} + \tfrac{1}{3} f_{3} \\
& + \tfrac{1}{3} f_{-3} - \tfrac{2}{21} f_{-4} + \tfrac{1}{3} \int_{x}^{\left(\frac{x^2}{h^2} - 1\right) h\,\%4} \Big|_{h} \Big|_{h+x}^{\tfrac{1}{2}} \\
& - \tfrac{2}{21} f_{-2} - \tfrac{2}{21} f_{0} - \tfrac{2}{21} f_{2} - \tfrac{2}{21} f_{4} - \tfrac{2}{21} f_{1} \\
& - \tfrac{2}{21} f_{-1} + \tfrac{1}{3} f_{3} + \tfrac{1}{3} f_{-3} - \tfrac{2}{21} f_{-4} \\
& + \tfrac{1}{3} \int_{x}^{\left(\frac{x^2}{h^2} - 1\right) h\,\%4} \Big|_{h} + \tfrac{1}{2} x \,\Big|_{h}^{\tfrac{2}{3}\frac{\%4}{h} - \tfrac{1}{3}\int_{x}^{\left(\frac{x^2}{h^2} - 1\right) h\,\%4} \Big|_{h}^{2}} \\
& + \tfrac{1}{3} \int_{x}^{\left(\frac{x^2}{h^2} - 1\right) h} \Big|_{h}^{\tfrac{1}{4}\frac{\%3}{h}} \\
& + \tfrac{1}{4} \int_{h}^{x} \left(x \,\Big|_{h}^{\tfrac{2}{5}\frac{\%2}{h} - \tfrac{1}{5}\int_{x}^{\left(\frac{x^2}{h^2} - 4\right) h\,\%2} \Big|_{h}^{2} + \tfrac{1}{30}\int_{x}^{\left(\frac{x^2}{h^2} - 4\right) \%1} \Big|_{h}^{2}} \right) \Big|_{h}^{x}
\end{aligned}
$$

$$\%1 := -\frac{2}{21} f[-6] - 2 f[-4] - \frac{12}{7} f[-2] + \frac{8}{3} f[-3] + \frac{5}{7} f[-5] + \frac{3}{7} f[1] - \frac{12}{7} f[2] + \frac{8}{3} f[3] - 2 f[4] + \frac{5}{7} f[5] - \frac{2}{21} f[6] + \frac{3}{7} f[-1]$$

$$\%2 := \frac{1}{2} d5y[-1/2] + \frac{1}{2} d5y[1/2] + \frac{1}{6} \frac{x\ \%1}{h}$$

$$\%3 := \frac{11}{21} f[-4] + \frac{3}{7} f[-2] - \frac{6}{7} f[-3] - \frac{2}{21} f[-5] + \frac{3}{7} f[2] - \frac{6}{7} f[3] + \frac{11}{21} f[4] - \frac{2}{21} f[5] + \frac{1}{5} \frac{\left(\frac{x^2}{h^2} - 4\right) h\ \%2}{x}$$

$$\%4 := \frac{1}{2} d3y[-1/2] + \frac{1}{2} d3y[1/2] + \frac{1}{4} \frac{x\ \%3}{h}$$

```
> Y2 := diff(Y1,x);
```

$$Y2 := 2 \left|\frac{1}{2}\right| - \frac{2}{21} f[-2] - \frac{2}{21} f[0] - \frac{2}{21} f[2] - \frac{2}{21} f[4] - \frac{2}{21} f[1] - \frac{2}{21} f[-1] + \frac{1}{3} f[3] + \frac{1}{3} f[-3] - \frac{2}{21} f[-4] + \frac{1}{3} \frac{\left(\frac{x^2}{h^2} - 1\right) h\ \%6}{x} \Big|_{/h}$$

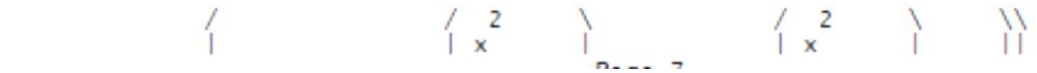

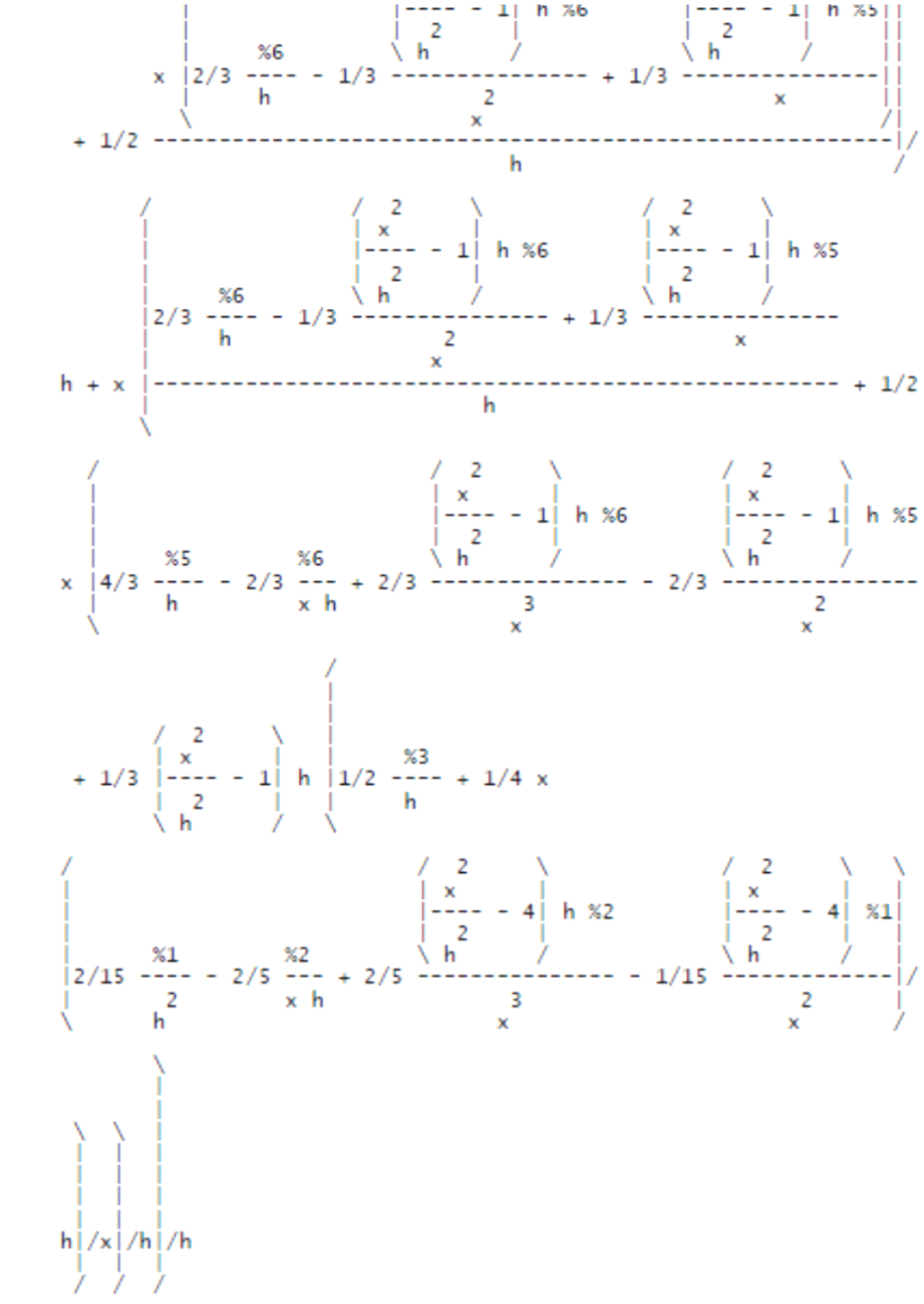

$$\%1 := -\frac{2}{21} f[-6] - 2 f[-4] - \frac{12}{7} f[-2] + \frac{8}{3} f[-3] + \frac{5}{7} f[-5] + \frac{3}{7} f[1] - \frac{12}{7} f[2] + \frac{8}{3} f[3] - 2 f[4] + \frac{5}{7} f[5]$$

```
      - 2/21 f[6] + 3/7 f[-1]

                                                          x %1
%2 := 1/2 d5y[-1/2] + 1/2 d5y[1/2] + 1/6 ----
                                           h

                      /  2     \              /  2     \
                      | x      |              | x      |
                      |---- - 4| h %2         |---- - 4| %1
                      |  2     |              |  2     |
             %2       \ h      /              \ h      /
%3 := 2/5 ---- - 1/5 ---------------- + 1/30 -------------
           h                  2                    x
                             x

      11
%4 := -- f[-4] + 3/7 f[-2] - 6/7 f[-3] - 2/21 f[-5] + 3/7 f[2]
      21

                                                 /  2     \
                                                 | x      |
                                                 |---- - 4| h %2
                                                 |  2     |
                                                 \ h      /
                    11
      - 6/7 f[3] + -- f[4] - 2/21 f[5] + 1/5 ----------------
                   21                              x

             %4          x %3
%5 := 1/4 ---- + 1/4 ----
           h           h

                                                          x %4
%6 := 1/2 d3y[-1/2] + 1/2 d3y[1/2] + 1/4 ----
                                           h

> simplify(Y1);

                                                  4                  4                  4
- 1/15120 (2268 f[-2] h  x + 1440 f[0] h  x + 2268 f[2] h  x

                  4                  4                  4
      + 2436 f[4] h  x + 1368 f[1] h  x + 1368 f[-1] h  x

                  4                  4                  4
      - 6568 f[3] h  x - 6568 f[-3] h  x + 2436 f[-4] h  x

             3      2          3      2          3      2
      - 2160 x  f[-4] h  - 1800 x  f[-2] h  + 3280 x  f[-3] h

             3      2          3      2          3      2
      + 540 x  f[-5] h  - 1800 x  f[2] h  + 3280 x  f[3] h

             3      2          3      2          4
      - 2160 x  f[4] h  + 540 x  f[5] h  - 315 x  d5y[-1/2] h

             4                  3  2               2  3
      - 315 x  d5y[1/2] h - 40 x  h  f[-6] + 945 x  h  d5y[-1/2]

             2  3                  3  2               3  2
      + 945 x  h  d5y[1/2] + 180 x  h  f[1] - 40 x  h  f[6]

            3  2               2            3         2           3
+ 180 x  h  f[-1] - 3780 x  d3y[-1/2] h  - 3780 x  d3y[1/2] h
```

```
      - 240 h^4 f[-5] x - 240 h^4 f[5] x + 16 h^4 x f[-6] + 16 h^4 x f[6]

      - 7560 dy[-1/2] h^5 - 7560 dy[1/2] h^5 + 12 x^5 f[-6]

      + 252 x^5 f[-4] + 216 x^5 f[-2] - 336 x^5 f[-3] - 90 x^5 f[-5]

      - 54 x^5 f[1] + 216 x^5 f[2] - 336 x^5 f[3] + 252 x^5 f[4]

      - 90 x^5 f[5] + 12 x^5 f[6] - 54 x^5 f[-1] - 252 h^5 d5y[-1/2]

      - 252 h^5 d5y[1/2] + 1260 h^5 d3y[-1/2] + 1260 h^5 d3y[1/2]) / h^6

> simplify(Y2);

- 1/7560 (-630 x^3 d5y[-1/2] h - 630 x^3 d5y[1/2] h - 60 x^2 h^2 f[-6]

      - 3240 x^2 h^2 f[-4] - 2700 x^2 h^2 f[-2] + 4920 x^2 h^2 f[-3]

      + 810 x^2 h^2 f[-5] + 270 x^2 h^2 f[1] - 2700 x^2 h^2 f[2]

      + 4920 x^2 h^2 f[3] - 3240 x^2 h^2 f[4] + 810 x^2 h^2 f[5]

      - 60 x^2 h^2 f[6] + 270 x^2 h^2 f[-1] + 945 h^3 x d5y[-1/2]

      + 945 h^3 x d5y[1/2] + 30 x^4 f[-6] - 225 x^4 f[5] - 135 x^4 f[-1]

      + 30 x^4 f[6] + 630 x^4 f[-4] + 540 x^4 f[-2] - 840 x^4 f[-3]

      - 225 x^4 f[-5] - 135 x^4 f[1] + 540 x^4 f[2] - 840 x^4 f[3]

      + 630 x^4 f[4] + 8 h^4 f[-6] + 1218 h^4 f[-4] + 1134 h^4 f[-2]

      - 3284 h^4 f[-3] - 120 h^4 f[-5] + 684 h^4 f[1] + 1134 h^4 f[2]

      - 3284 h^4 f[3] + 1218 h^4 f[4] - 120 h^4 f[5] + 8 h^4 f[6]

      + 684 h^4 f[-1] - 3780 x d3y[-1/2] h^3 - 3780 x d3y[1/2] h^3

      + 720 f[0] h^4 ) / h^6
```

```
> x := 0;
                                  x := 0
> dY := simplify("""");
dY := - 1/60 (-30 dy[-1/2] - 30 dy[1/2] - d5y[-1/2] - d5y[1/2]
     + 5 d3y[-1/2] + 5 d3y[1/2])/h
> ddy := simplify("""");
ddy := - 1/3780 (4 f[-6] + 609 f[-4] + 567 f[-2] - 1642 f[-3]
     - 60 f[-5] + 342 f[1] + 567 f[2] - 1642 f[3] + 609 f[4]
                                                          2
     - 60 f[5] + 4 f[6] + 342 f[-1] + 360 f[0])/h
> for j from -5 to 5 do f[j-1] := 2*f[j] - f[j+1] + d2y[j]; od;
                  f[-6] := 2 f[-5] - f[-4] + d2y[-5]

                  f[-5] := 2 f[-4] - f[-3] + d2y[-4]

                  f[-4] := 2 f[-3] - f[-2] + d2y[-3]

                  f[-3] := 2 f[-2] - f[-1] + d2y[-2]

                  f[-2] := 2 f[-1] - f[0] + d2y[-1]

                   f[-1] := 2 f[0] - f[1] + d2y[0]

                    f[0] := 2 f[1] - f[2] + d2y[1]

                    f[1] := 2 f[2] - f[3] + d2y[2]

                    f[2] := 2 f[3] - f[4] + d2y[3]

                    f[3] := 2 f[4] - f[5] + d2y[4]

                    f[4] := 2 f[5] - f[6] + d2y[5]
> simplify(dY);
- 1/60 (-30 dy[-1/2] - 30 dy[1/2] - d5y[-1/2] - d5y[1/2]
     + 5 d3y[-1/2] + 5 d3y[1/2])/h
> d3y[-1/2] := dy[1/2] - 2*dy[-1/2] + dy[-3/2];
             d3y[-1/2] := dy[1/2] - 2 dy[-1/2] + dy[-3/2]
```

```
> d3y[1/2] := dy[3/2] - 2*dy[1/2] + dy[-1/2];
                d3y[1/2] := dy[3/2] - 2 dy[1/2] + dy[-1/2]
> d5y[1/2] := dy[5/2] - 4*dy[3/2] + 6*dy[1/2] - 4*dy[-1/2] + dy[-3/2];
 d5y[1/2] := dy[5/2] - 4 dy[3/2] + 6 dy[1/2] - 4 dy[-1/2] + dy[-3/2]
> d5y[-1/2] := dy[3/2] - 4*dy[1/2] + 6*dy[-1/2] - 4*dy[-3/2] + dy[-5/2];
d5y[-1/2] := dy[3/2] - 4 dy[1/2] + 6 dy[-1/2] - 4 dy[-3/2] + dy[-5/2]
> dY;
- 1/60 (-37 dy[-1/2] - 37 dy[1/2] + 8 dy[3/2] + 8 dy[-3/2] - dy[-5/2]
      - dy[5/2])/h
```